INTRODUCTION

The electronic transport properties in disordered semiconductors in the strong scattering regime are reported with special focus on the study of the dc conductivity and thermopower in these materials. The model that is developed here should be applicable to liquid or amorphous semiconductors with sufficiently wide energy gaps.

In intrinsic semiconductors there are only two bands that affect transport properties, an empty conduction band and a filled valence band, and there are no states in the energy gap between them. The conductivity is then due to thermal excitation across the gap and is usually expressed

$$\sigma(T) = \sigma_0 \exp(-\Delta E / k_B T), \tag{1.1}$$

where ΔE is the activation energy which is equal to half of the energy gap. σ_0 is a prefactor which is related to the mobility of the charge carriers (electrons and holes) and is usually taken as constant for each material.

For amorphous, liquid, and doped semiconductors, Equation 1.1 is not suitable because in these materials, in addition to the states in the conduction and valence bands, the host bands, there are usually many states lying in the gap. Electrons or holes in these states my contribute to the conductivity in several ways. First, if the concentration of gap states is sufficient, they can form a narrow band and carriers can tunnel from state to state. Secondly, if the temperature is high enough, carriers can be thermally excited to or from one of the host bands but with an activation energy unrelated to the gap width. Thus one finds that the conductivity in doped semiconductors depends strongly on temperature and impurity concentration.

It is well known that in amorphous semiconductors, there exist many broken bonds and that these broken bonds often produce states within the gap. These defect states may be quite similar to the impurity states in doped semiconductors. The accepted model for liquid semiconductors is that its structure is dominated by a covalent bond network in which the bonds are continually breaking and reforming, so that at any point in time there exist many broken bonds. The states associated with these broken bonds may also lie within the gap. Unlike amorphous and doped semiconductors,

1

however, where the concentration of broken bonds and impurities does not strongly depend on temperature, in liquid semiconductors, the broken bond concentration should depend strongly on temperature.

Defects, broken bonds, and impurities all affect transport properties in disordered semiconductors because all create states within the gap. Because of this similarity, the words "defect" states or "defect" band are often used as generic terms to represent any and all of these effects.

A simple model to describe the electronic transport properties in liquid and amorphous semiconductors has been investigated. In this model only two bands, the defect and host bands, are included so that it is only necessary to introduce two different site energies, one for an electron (or hole) at a host site and the other for an electron (or hole) at a defect site. This approximation is only applicable for materials with wide gaps, so this work is confined to such materials. The energies associated with individual sites shift due to the interaction between overlapping states at neighboring sites. This overlapping of the states also allows electrons to hop from site to site. There are three types of hopping that can occur: *host site* ⇌ *host site, defect site* ⇌ *defect site*, and *defect site* ⇌ *host site*. In the calculation reported here, these three types of hopping are represented by three different hopping integrals, which may or may not have the same values.

In addition to the site energies and hopping integrals, another very important parameter is the temperature. In previous theoretical work, temperature effects were usually treated using Maxwell-Boltzmann statistics. At high temperature or when the defect states lie close to a host band, this approximation is very poor, and it is important to use Fermi-Dirac statistics and to include the shift of chemical potential with temperature. The careful analysis of this shift in the chemical potential is an essential contribution of the work reported here.

The effect of the defect concentration on transport properties has also been investigated thoroughly and is reported in this work. The results show that the conductivity has a complex dependence on defect concentration, the position of the defect band with respect to host band, and temperature. When the defect concentration is very low, the defect states are all localized and do not spread out into a band. With increasing concentration, these states become extended and the mobility of the carriers increases. The concentration at which this increase in mobility occurs depends strongly on the energy separation between the host and defect bands. If this separation between the bands is small, the bands will begin to overlap even at low defect concentration. In this case the conductivity will have important contributions both from the carriers in the defect band and those that are excited

into the host band. If the separation between the two bands is larger, the mobility of the defect states remains low until the defect concentration is quite large. In this case, unless the temperature is extremely high, the conductivity will be almost entirely due to carriers in the defect band. These two cases are shown schematically in Figure 1.1. Figure 1.1a shows the bands when the defect concentration is quite low and the states are all localized. Figure 1.1b shows extended states in the defect band due to the bands overlapping, while Figure 1.1c shows that extended states have formed as the concentration of the defect band itself has increased.
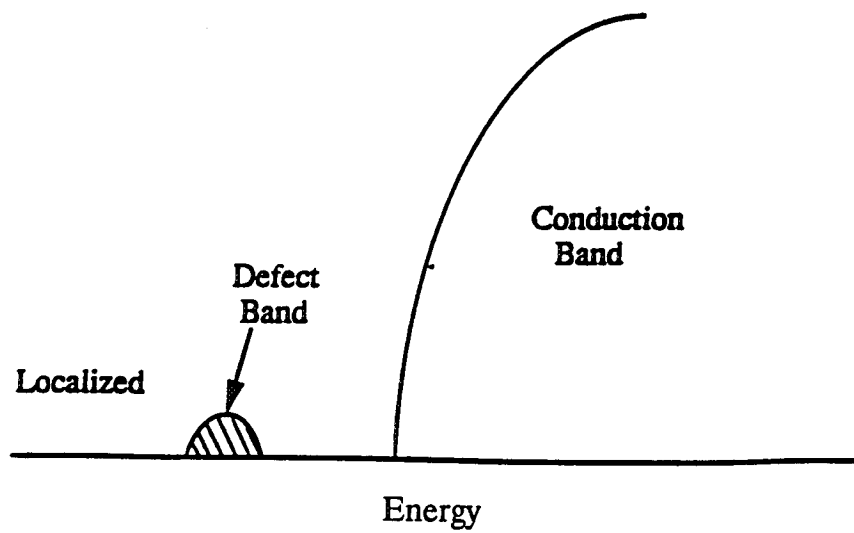
Figure 1.1a Schematical position of conduction band and localized defect band.
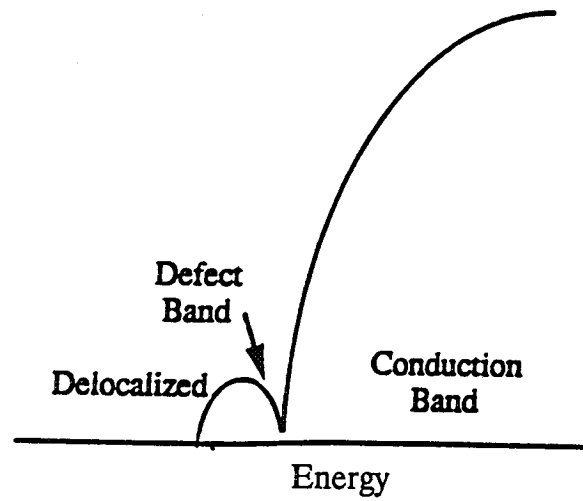
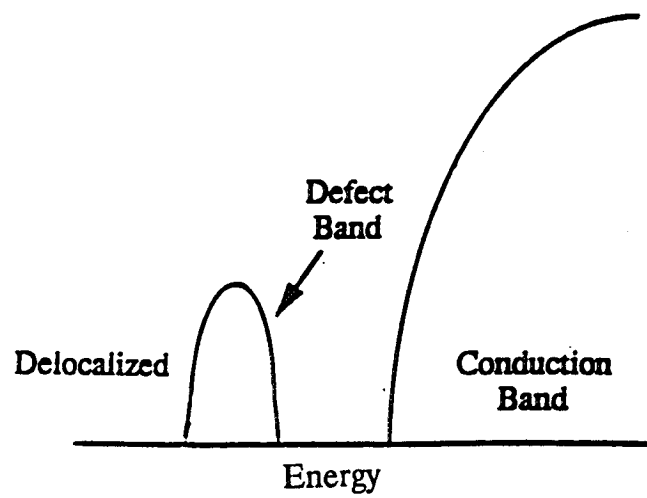Figure 1.1b States in defect band are delocalized as overlap increases

Figure 1.1c States in defect band are delocalized when defect concentration increases.

NUMERICAL RESULTS

2.1. Density of States $\rho(E)$ and Energy-Dependent Conductivity $\sigma(E)$

Figure 2.1 shows the calculated plots of the density of states (DOS) of the defect and host bands for different defect concentrations, x, and site energy differences, $\Delta\varepsilon$. As mentioned in Chapter I, the effect of the valence band has been neglected. In these curves the site energy of the host band is taken to be zero, and all other energies are measured with respect to it. It can be seen that with increasing defect concentration, the defect band grows while the host band decreases. To see how the two schematic models described in Chapter I work, DOS curves are shown for the two cases described there. Figure 2.1a shows the case with a large site-energy difference, $\Delta\varepsilon=1.1\ eV$. Here there is little overlap between the defect and the host bands for $x=0.06$, but the overlap can be seen to increase for $x=0.12$. On the other hand, in Figure 2.1b with a smaller site energy difference, $\Delta\varepsilon=0.85\ eV$, the overlap is appreciable even at $x=0.06$. From these graphs, we can see that greater overlap can be achieved in two ways; one is by increasing the defect concentration, while the other is by decreasing the site-energy difference.

The defect band filling factor, $r\ (\ 0\ \le r\ \le 2.0)$, is defined as the ratio of the number of electrons to the number of states in the defect band. When all the states in defect band are occupied, $r=2.0$, while when it is empty, $r=0$. The Fermi energy is the zero temperature chemical potential $\mu(0)$. The values of $\mu(0)$ for $r = 1.0$, 1.5, and 2.0 for $x=0.06$ are given in Table 2.1.

Table 2.1 Zero temperature chemical potential $\mu(0)$ for $x=0.06$

	$\mu(0)^{[a]}[eV]$	$\mu(0)^{[b]}[eV]$
r=1.0	-1.34	-1.50
r=1.5	-1.27	-1.43
r=2.0	-1.16	-1.19

[a] $\Delta\varepsilon = 0.85\ eV$
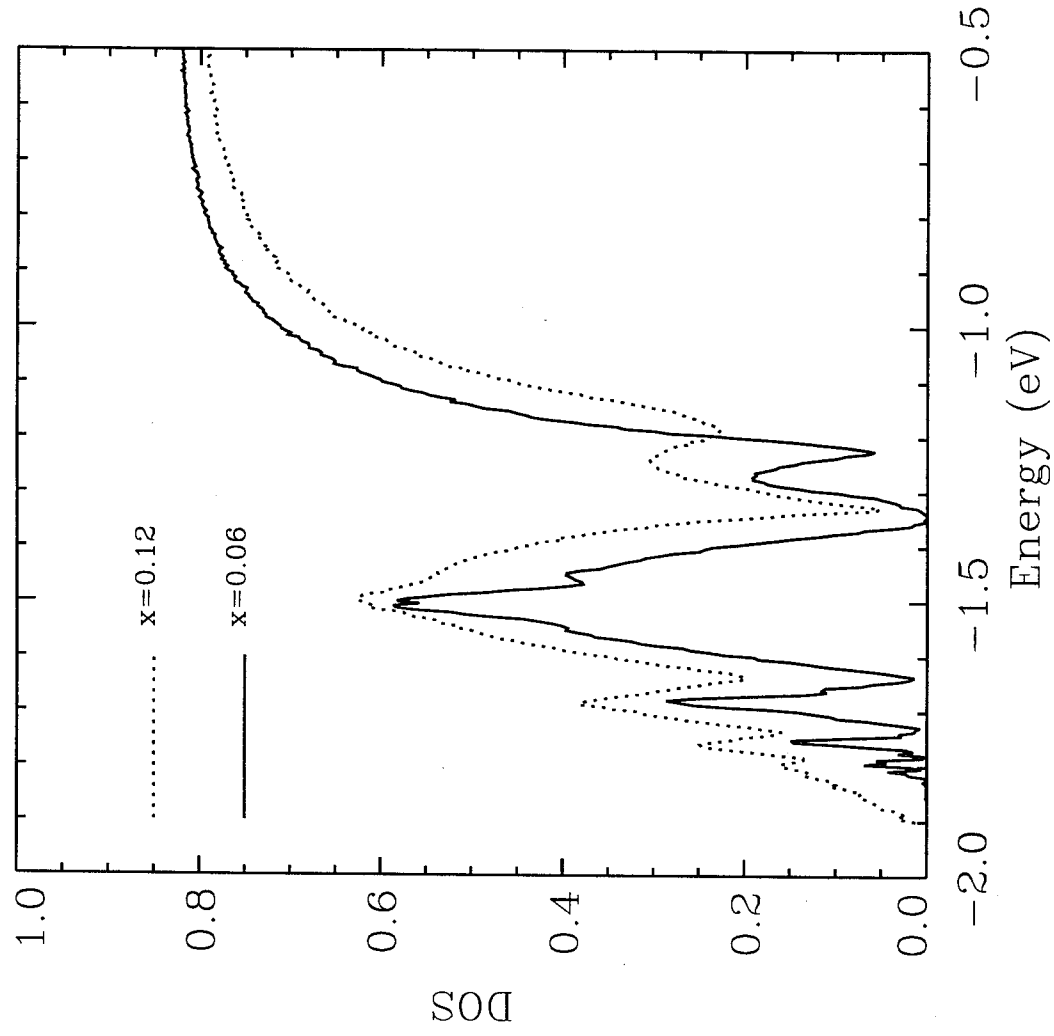[b] $\Delta\varepsilon = 1.1\ eV$.

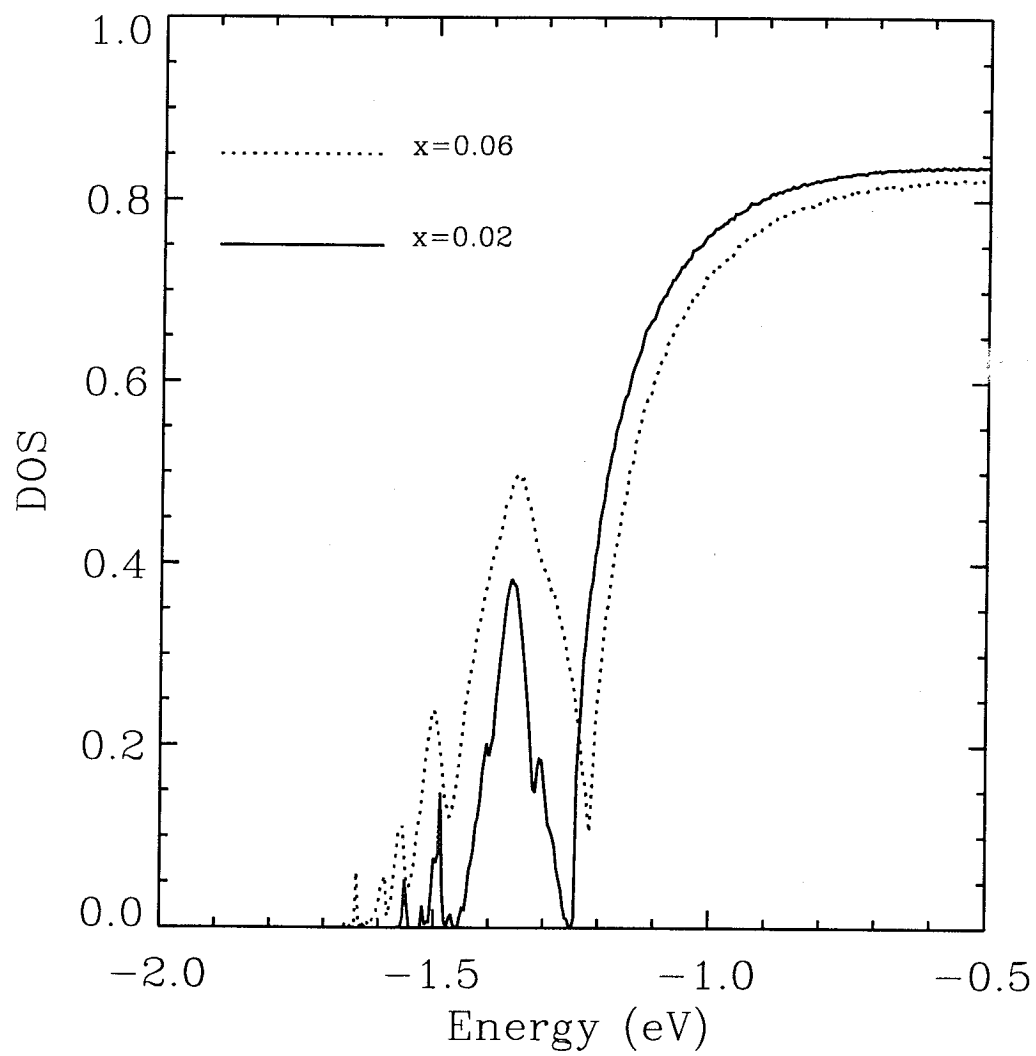Figure 2.1a DOS curve for $\Delta\epsilon = 1.1$ eV

Figure 2.1b DOS curve for $\Delta\epsilon$ = 0.85 eV

Unlike the usual schematic drawing of an defect band, the calculated band contains a number of sharp peaks. These peaks are caused by clusters of 1, 2, 3, or more defect atoms surrounded by host atoms. These sharp peaks are clearly resolved at low concentrations where there is a large probability for defect atoms to be surrounded by host atoms. In Figure 1b the side peaks on the left side of the defect band are pronounced while those on the right side ones have merged with the host band. The DOS for a very large site-energy difference, $\Delta\varepsilon=1.9\ eV$, is shown in Figure 2.2 for $x=0.10$. In this graph the sharp peaks are even more pronounced. This is because when the neighboring band separation is larger the electrons at defect sites have less interaction with electrons at host sites, and thus are more nearly localized.

Figure 2.3 shows the energy-dependent conductivity $\sigma(E)$ for the same values of x as in Figure 2.1. In Figure 2.3a, $\Delta\varepsilon = 1.1\ eV$, while in Figure 2.3b, $\Delta\varepsilon = 0.85\ eV$. By comparing the two curves with $x=0.06$, one can see that for energies in the region of defect band, $\sigma(E)$ is somewhat larger when the defect band overlaps with the host band. In addition, the sharp peaks that were evident in the DOS curves have almost disappeared. This is because the states contributed by small clusters of defect atoms that form the sharp peaks in the DOS have very low mobility, and thus they make only a small contribution to the conductivity.

2.2. Repulsion between the Defect Band and Host Band.

We know from quantum mechanics that closely-spaced energy bands repel each other when there is an interaction that couples them. In our band model, the energy bands are coupled by the hopping term in the Hamiltonian, so we expect that the bands to repel each other.

In both Figure 2.1a and 2.1b, the defect band is easily distinguished from the host band even though the energy difference between the host and defect sites has been taken to be less than or equal to half of the host band width, 1.1 eV. This is due to the effect of band repulsion. Figure 2.4 shows the calculated band repulsion, Γ, between the host and defect bands as a function of site energy difference $\Delta\varepsilon$ for $x=0.1$. Here Γ is defined as the difference between the energy separation of the centers of the two bands and $\Delta\varepsilon$. As expected the band repulsion is zero when the site energies for host and defect atoms are the identical, i. e., $\Delta\varepsilon=0$, and when the separation is very large, that is $\Delta\varepsilon\to\infty$. We find that for low defect concentration, the repulsion is a maximum when $\Delta\varepsilon$ is close the
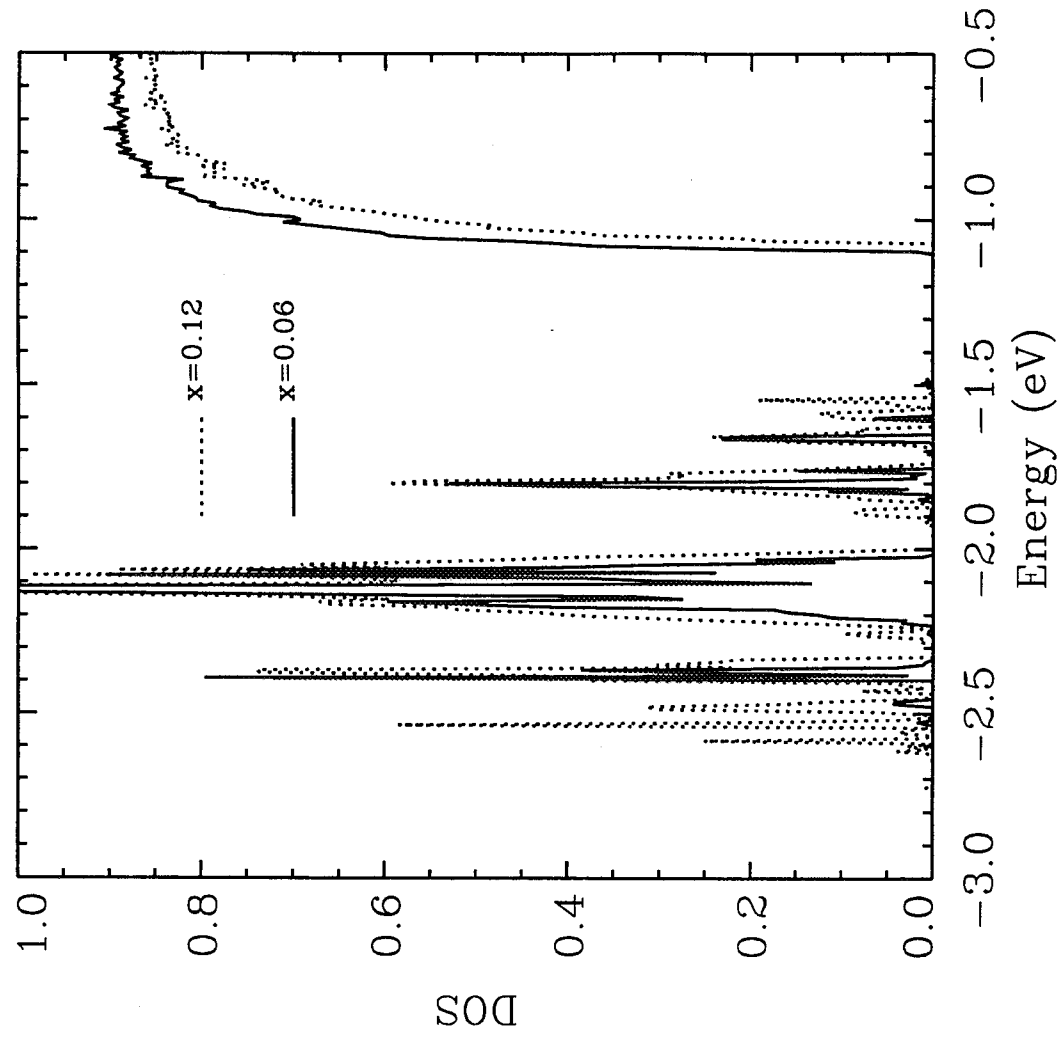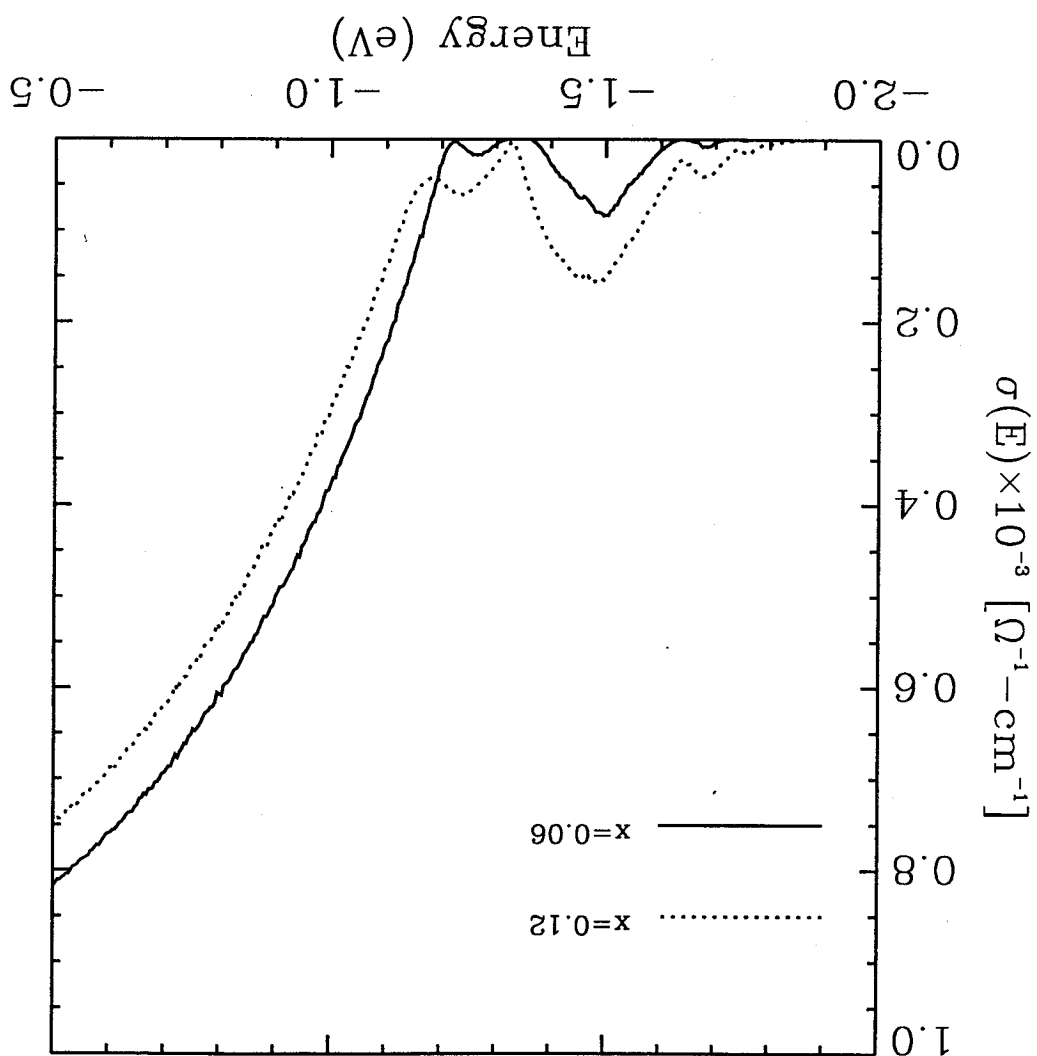
Figure 2.2 DOS curve for Δε = 1.9 eV

Figure 2.3a Energy-dependent conductivity for $\Delta\varepsilon = 1.1$ eV

Energy (eV)

−0.5   −1.0   −1.5   −2.0

$\sigma(E)\times10^{-3}$ $[\Omega^{-1}-\mathrm{cm}^{-1}]$
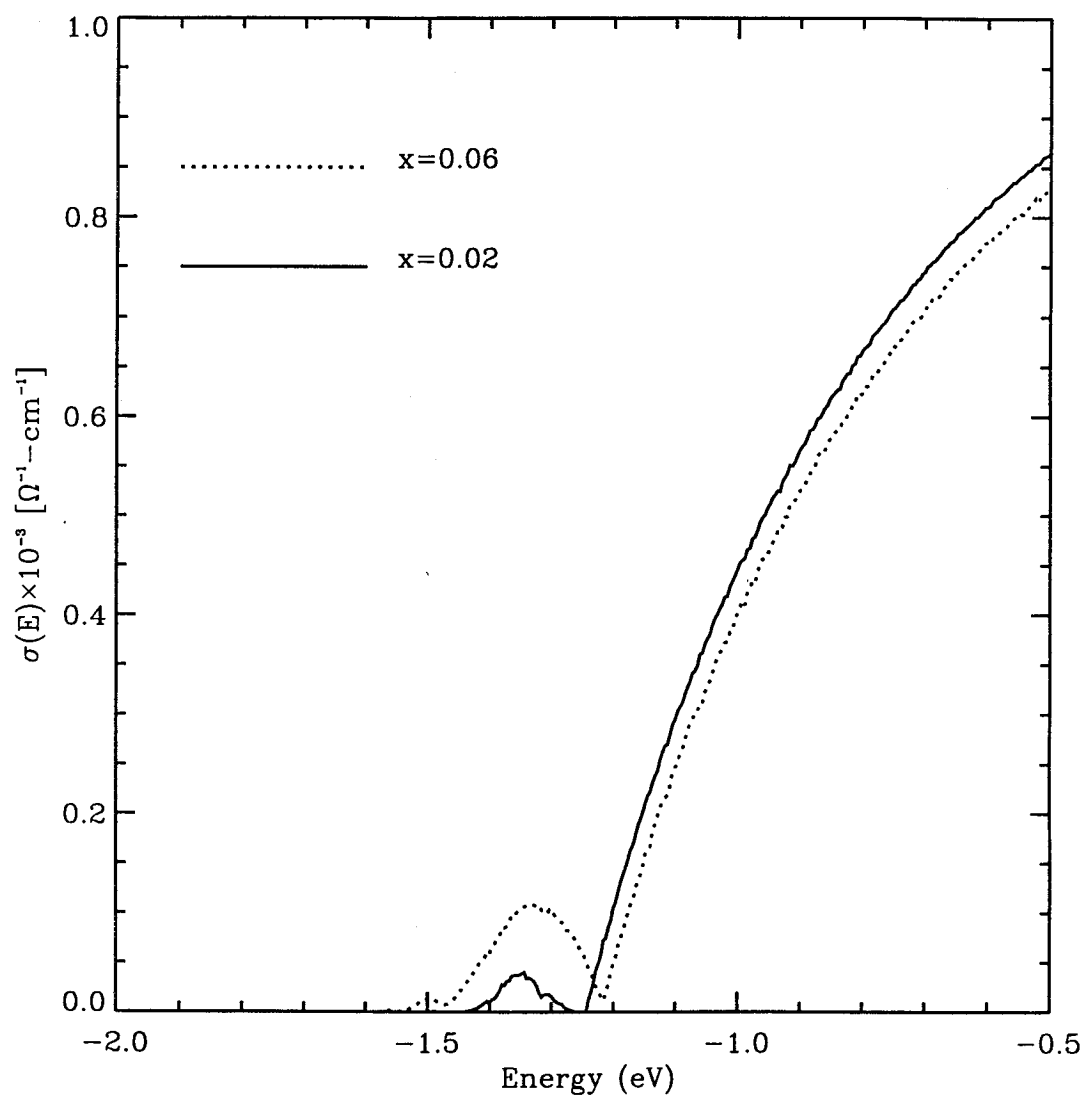
0.0   0.2   0.4   0.6   0.8   1.0

x=0.06

x=0.12

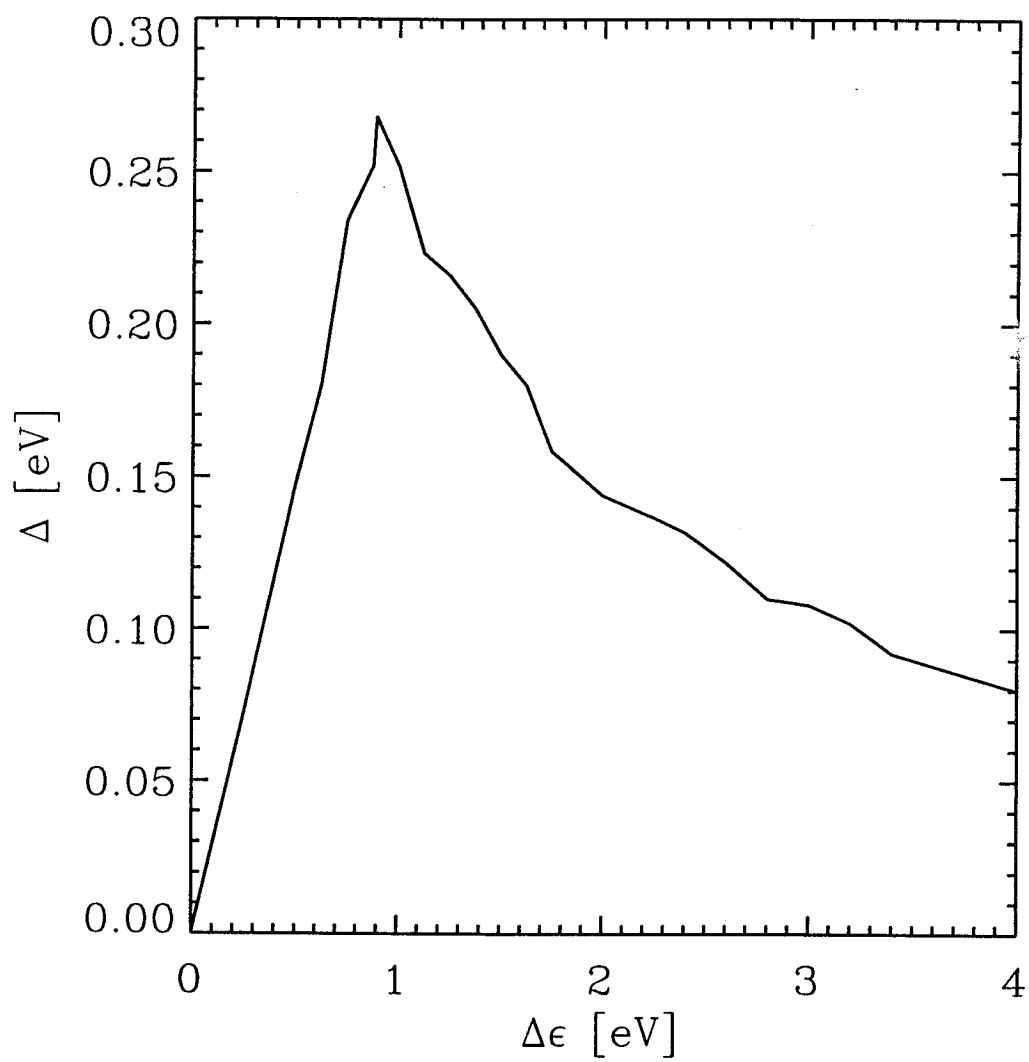Figure 2.3b Energy−dependent conductivity for $\Delta\epsilon$ =0.85 eV

Figure 2.4 Band repulsion as a function of $\Delta\epsilon$

host band width, i.e, just when the defect band would be expected to emerge from within the host band. In Figure 2.4, the repulsion is maximum for $\Delta \varepsilon = 0.9\ eV$. For larger values of the site energy difference, the repulsion falls off as $1/\Delta \varepsilon$. This dependence on $\Delta \varepsilon$ can be deduced from an analytical investigation of a model sample with only two sites. In this case the expression for the level repulsion is found to be $\Gamma = 2t^2/\Delta \varepsilon$. Since the repulsion for defect states should be roughly proportional to the number of the nearest neighbors, it is reasonable that the band repulsion should be given by $\Gamma = 2Kt^2/\Delta \varepsilon$. For $\Delta \varepsilon/t > 10$ our calculated results fit this expression quite well. Table 2.2 is a comparison of the repulsion obtained from our numerical calculations and the repulsion obtained from the simple equation above. It can be seen that the agreement is excellent.

For the low defect concentrations shown in Figure 2.1, the center of the host band remains close to the host site energy, while the shift mainly comes from the defect band. This is because the shift for each type of atom depends on the fraction of neighbors of the opposite type. On the average, each defect atom has many more host atom neighbors than vice versa.

Table 2.2 Comparison of numerically and analytically calculated band repulsion.

$\varepsilon_a - \varepsilon_b$	$(\varepsilon_a - \varepsilon_b)/t_{ab}$	Repulsion(Γ)	$2Kt_{ab}^2/(\varepsilon_a - \varepsilon_b)$
2.4	12	0.132	0.133
2.6	13	0.120	0.123
2.8	14	0.110	0.114
3.0	15	0.108	0.106
3.2	16	0.100	0.100
3.4	17	0.092	0.094
3.6	18	0.088	0.089
3.8	19	0.084	0.084
4.0	20	0.080	0.080

2.3. Shift of the Chemical Potential $\mu(T)$ with Temperature

The value of the chemical potential is very important for calculating the transport properties of semiconducting materials. In order to get a better understanding of transport in semiconductors, the behavior of the chemical potential as a function of temperature needs to be known.

For intrinsic semiconductors, the Fermi energy lies in the gap between the conduction and valence bands. If the two bands have identical curvature, we can show analytically that the chemical potential is only weakly dependent on temperature. In most semiconductors, an impurity or defect band exists in the gap. The Fermi energy then can be either in the defect band or in the gap. We considered three different positions of the Fermi energy; at the center of the defect band (half-filled defect band), $r=1.0$, on the edge of the defect band, $r=1.5$, and in the gap between the defect band and host band, $r = 2.0$.

Figure 2.5 is a plot of $\mu(T)-\mu(0)$ v.s. $\mu(0)$ for $\Delta\varepsilon=0.85\ eV$, $x=0.06$, and $T = 300,\ 600$, and $900\ K$. To see how values of $\mu(0)$ correspond to positions within the defect band, refer back to Figure 2.1b. It can be seen that the shift of $\mu(T)$ is similar to the model calculation described in chapter IV. When $\mu(0)$ lies in the lower part of the defect band, the shift in $\mu(T)$ is clearly negative. With increasing $\mu(0)$, the direction of the shift changes. The turning point is slightly to the left of the center of the defect band. This is because the interaction between the host and defect bands makes the defect band asymmetric. With increasing temperature, the amount of the shift increases, and the turning point also shifts. In the gap region, the direction of the shift is determined by a competition between the two bands. We can see that at the upper defect band edge, there is a positive shift, while when $\mu(0)$ lies near the host band edge, there is a negative shift. The bumps on the curves are caused by the peaks in the DOS of the defect band.

Figure 2.6 shows the calculated $\mu(T)-\mu(0)$ as a function of temperature for three different values of $\mu(0)$ ($r=1.0$, 1.5, and 2.0), $x=0.02$, and $\Delta\varepsilon=0.85\ eV$. At low temperature, the shift in each case is small. With increasing temperature the behavior of each of the curves becomes quite distinct.

For $r=2.0$, $\mu(T)$ always shifts in a negative direction, but there is a temperature region where the slope of the curve decreases with temperature. Because $\mu(0)$ lies in the gap in this case, the shift is the sum of the contributions from the two bands, host band and defect band. The host band induces a negative shift in $\mu(T)$, while the defect band induces a positive shift in $\mu(T)$. Since $\mu(T)$ lies closer to the host band than the defect band, at low temperature the defect band has negligible effect. At higher temperature, the rate at which the shift occurs decreases as the effect of the defect band
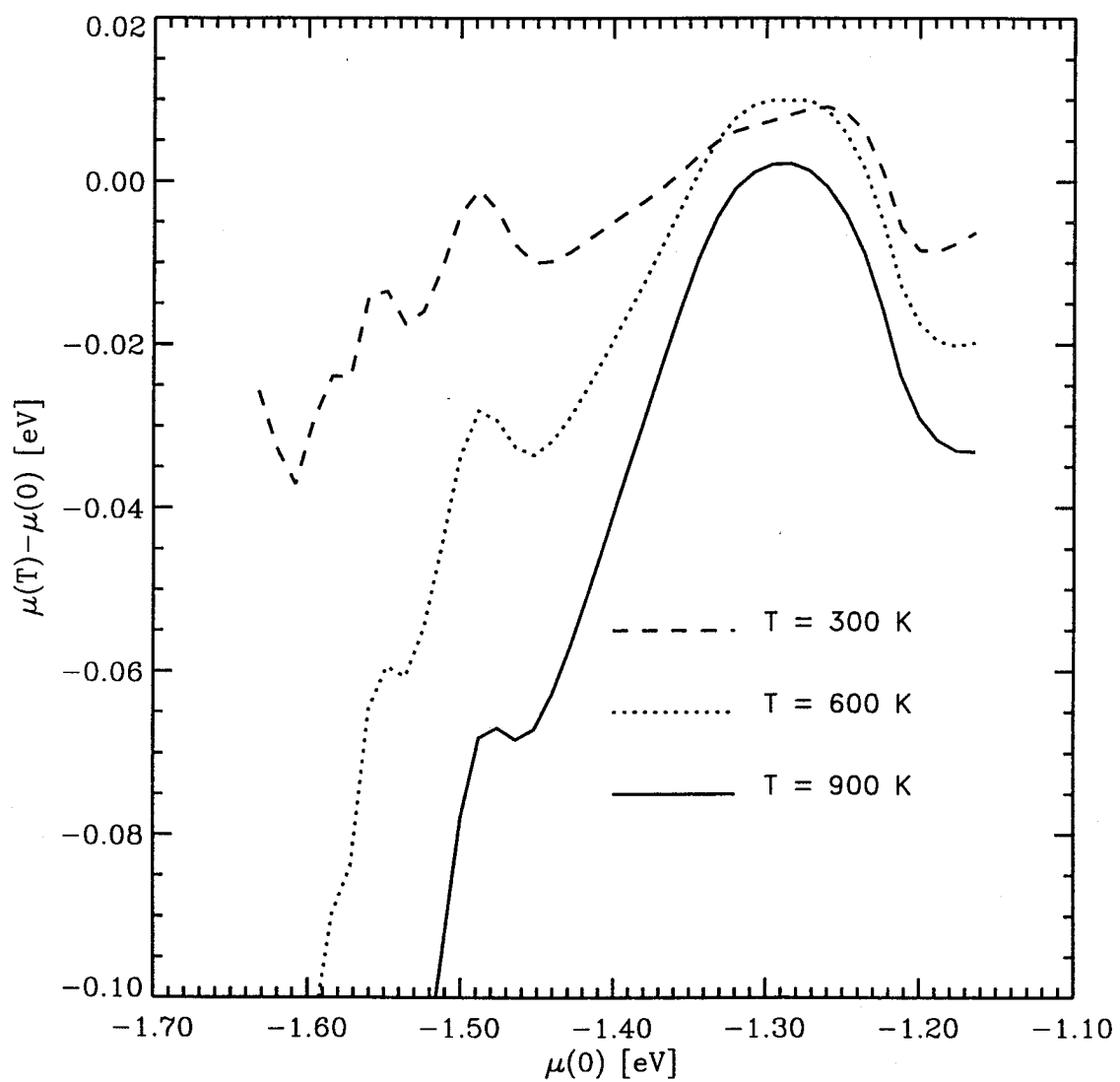
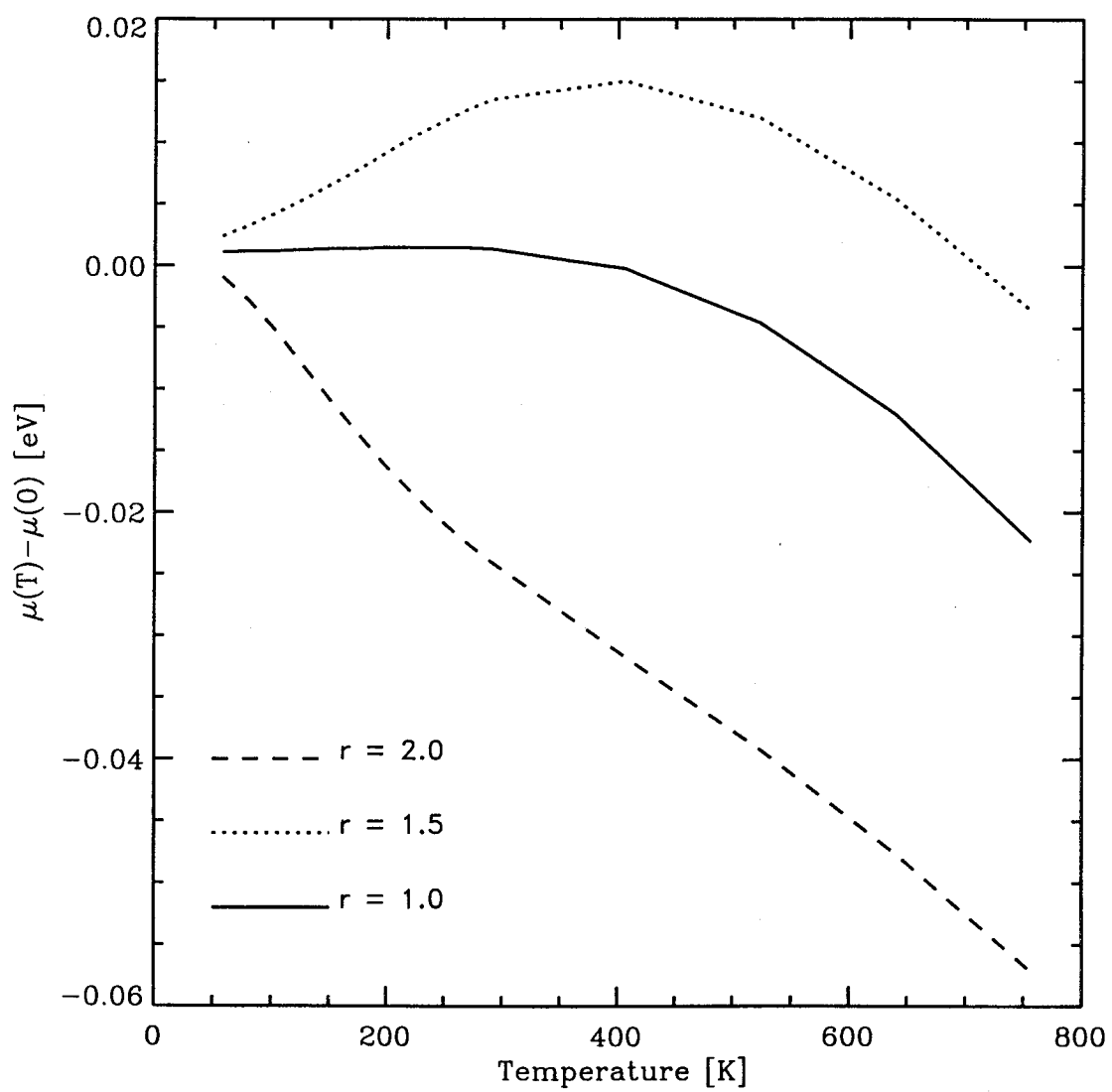Figure 2.5 Shift of μ at constant T for $\Delta\epsilon = 0.85$ eV

Figure 2.6 Shift of $\mu(T)$ as a function T for $\Delta\epsilon = 0.85$ eV x=0.02

increases. At even higher temperatures, the contribution from the defect band saturates but the part from the host band continues to increase.

For $r=1.0$, $\mu(T)$ remains essentially unchanged at low temperature. This is because in this case the defect band is half filled, and $\mu(0)$ lies at the center of the defect band. At low temperatures, the host band has negligible effect, and the defect band is quite symmetric in the neighborhood of $\mu(0)$. At higher temperature, $\mu(T)$ shifts to the negative direction because, with increasing temperature, the host band starts to have an effect. The temperature T at which $\mu(T)$ starts to shift approximately satisfies the relation $kT_{sh}=[E_c-\mu(0)]/3$, where E_c is the host band edge. In this figure, we can see that $T_{sh}=400\,K$.

The shift of $\mu(T)$ with temperature also depends on the site energy separation $\Delta\varepsilon$. Figure 2.7 shows $\mu(T)-\mu(0)$ as a function of T for $r=1.0$, $x=0.02$ and two values of $\Delta\varepsilon$, $\Delta\varepsilon=1.1\,eV$ and 0.85 eV. The vertical scale has been expanded by a factor of 4. We can see that the temperature at which $\mu(T)$ starts to shift in the negative direction depends strongly on $\Delta\varepsilon$. For $\Delta\varepsilon=1.1\,eV$, $T_{sh}\approx 700\,K$, while for $\Delta\varepsilon=0.85\,eV$, $T_{sh}\approx 400\,K$.

The most interesting case is in Figure 2.6 $r=1.5$, where $\mu(T)$ first experiences a positive shift then shifts in the negative direction. As before, at low temperature only the defect band has an effect, but in this case the DOS is extremely asymmetric around $\mu(0)$, which makes the shift very sensitive to temperature. At higher temperatures ($T > 700\,K$), the effect of the host band becomes important, which shifts $\mu(T)$ in other direction. Because the defect concentration is low, the contribution from the host band will finally dominate the shift. The temperature at which the shift in μ(T) changes sign will, of course, depend on both $\mu(0)$ and the defect concentration.

In Figure 2.8, we show $[\mu(T)-\mu(0)]$ as a function of T for three defect concentration, $x=0.01$, 0.03, and 0.05. Here $\mu(0)$ is on the edge of the defect band ($r = 1.5$) and $\Delta\varepsilon = 0.85\,eV$. We can see that the temperature at which the shift in $\mu(T)$ changes direction increases with defect concentration. This is because the defect band has a larger effect when the concentration is higher.

2.4. The dc Conductivity $\sigma(T)$

The calculation of the dc conductivity, $\sigma(T)$, is one of the main purposes of this project. Our calculation starts from the Kubo-Greenwood equation, and includes the temperature dependence of the chemical potential, $\mu(T)$, and the distribution function, $f(T)$. In liquid semiconductors we expect
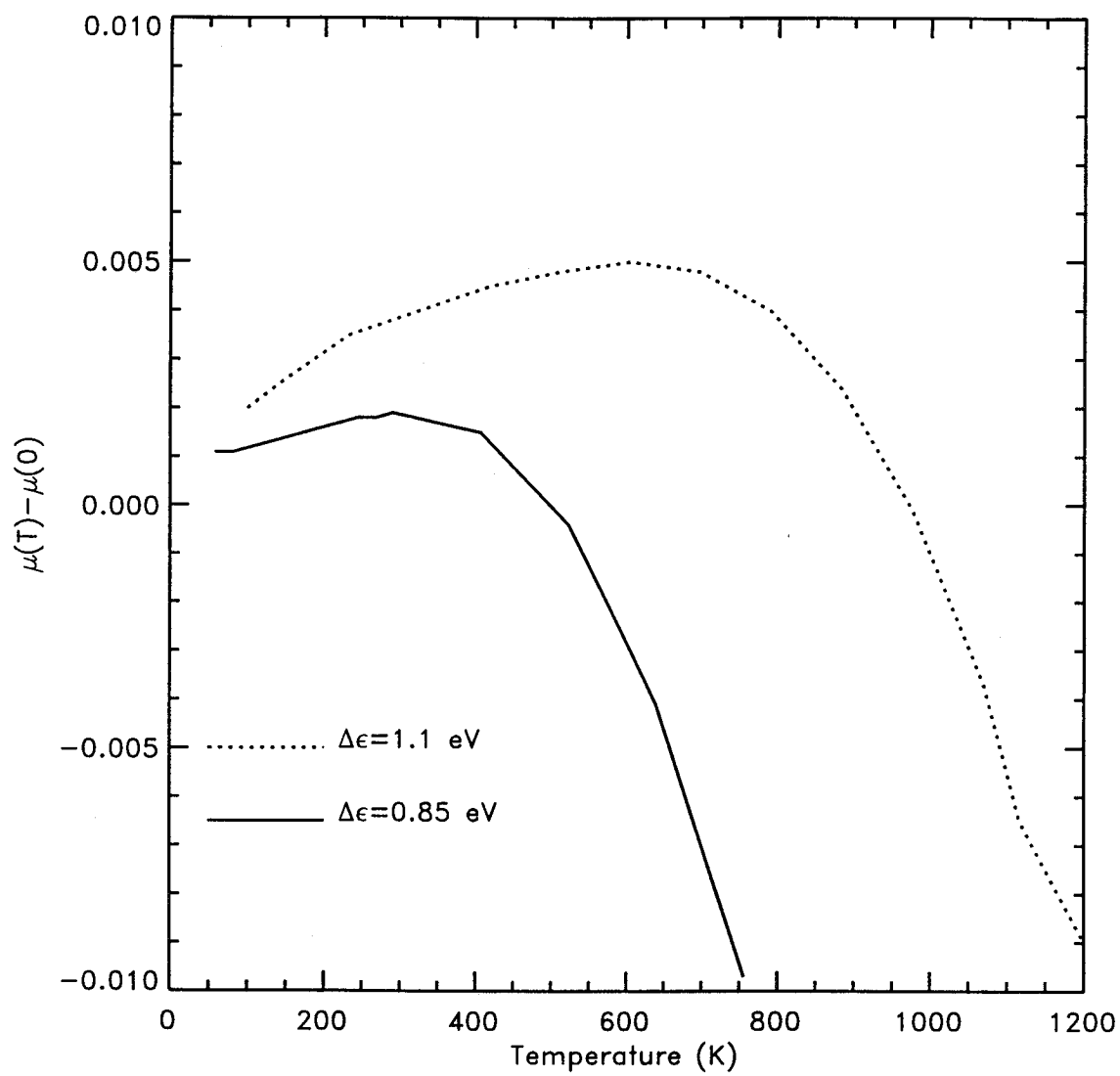
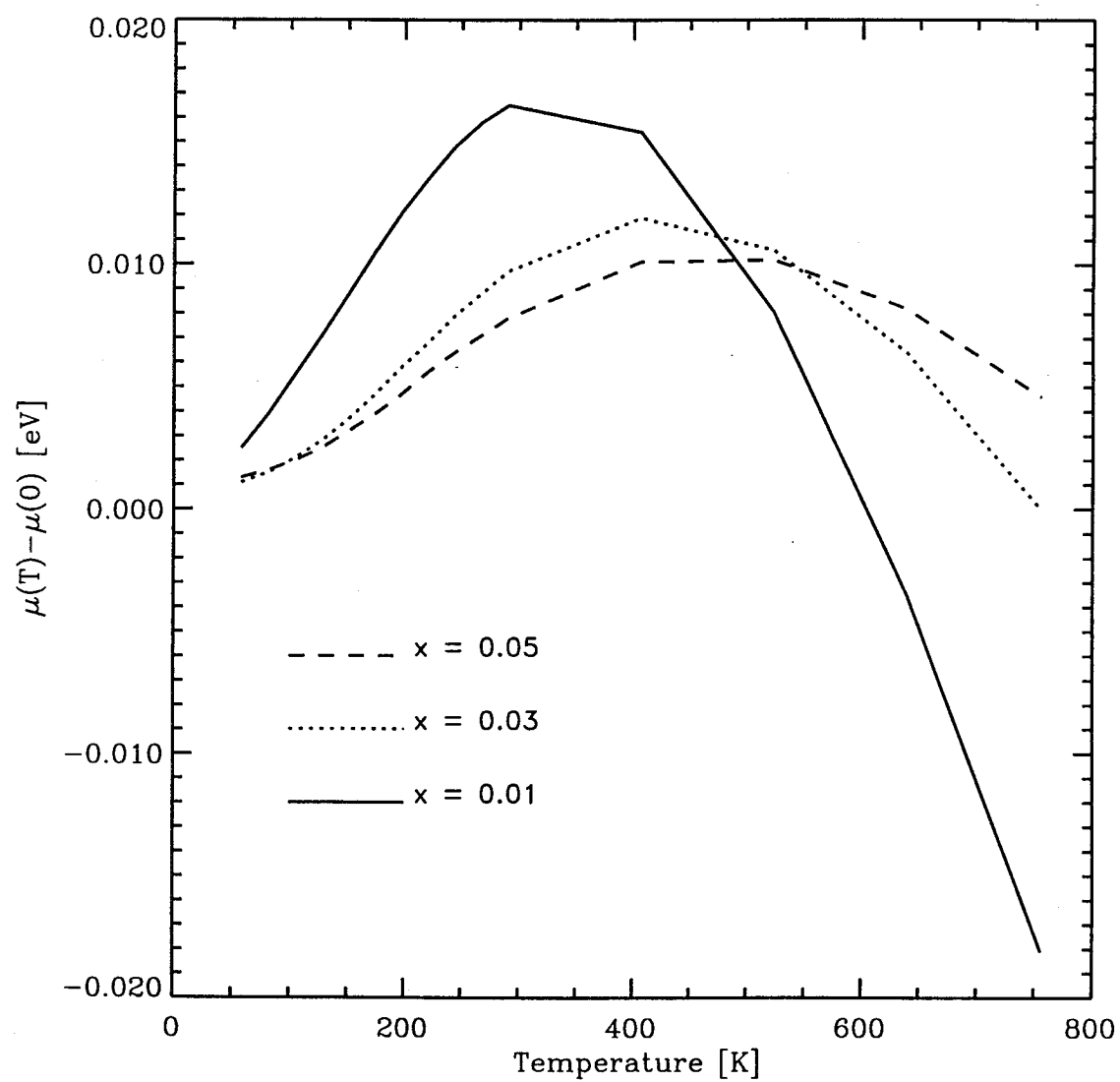Figure 2.7 Chemical potential as a function of T,r = 1.0, x=0.02

Figure 2.8 Shift of $\mu(T)$ as a function T for $\Delta\epsilon= 0.85$ eV r=1.5

a higher defect concentration due to the number of broken bonds which increase rapidly with T above the melting point.

$$\sigma = n e \mu_m(x),$$ (2.1)

Figure 2.9a and Figure 2.9b show the dc conductivity as a function of concentration at T=0 for three values of $\mu(0)$ (r=1.0, 1.5, and 2.0) for $\Delta\varepsilon=0.85\ eV$ and 1.1 eV, respectively. One can see that for r=1.5 and 2.0 at low concentrations the conductivity increases at a slower rate than at high concentrations in both cases. It is easier to understand the conductivity in terms of average mobility $\mu_m(x)$ of the defect band, generally one has where n is the number of carriers in the defect band, which should be proportional to the defect concentration, x. If $\mu_m(x)$ were constant, then the conductivity should increase be proportional to x. For $r = 1.0$, this is approximately true. However for $r = 1.5$ and 2.0, one can see that there is an increase in average mobility with concentration. For $r=1.5$, where $\mu(0)$ is on the edge of the defect band, the figure indicates that the average mobility of the carriers begins to increase at about 2% for $\Delta\varepsilon = 0.85$ and at about 15%. For $r=2.0$, $\mu(0)$ is in the gap causing the DOS at $\mu(0)$ to be very small compared to the other two cases. Here the increase in carrier mobility is mainly due to the increasing overlap of the defect and host bands, which occurs with increasing defect concentration.

Semiconductors are usually used in the temperature range T ≥ 300 K so the T=0 results must be generalized. For T > 0, activation of carriers to the host band has a large effect on $\sigma(T)$. The temperature-dependent chemical potential is very important in calculating $\sigma(T)$. Since the behavior of $\mu(T)$ is very different for different values of $\mu(0)$, we expect to see quite different behavior in $\sigma(T)$ for different values of $\mu(0)$.

In Figure 2.10a and Figure 2.10b we plot $\sigma(T)$ as a function of T for $\Delta\varepsilon=0.85$ and 1.1 eV at $x=0.02$. One can see that for r=1.0 and 1.5, the conductivity first decreases with T, while at higher temperature, it begins to increase with T. The fact that the conductivity first decreases with temperature contradicts our expectation since conduction in most semiconductors is dominated by the activation of carriers with temperature. The reasons for this unusual behavior is due to the behavior of the shift of $\mu(T)$ (See Figure 2.6.). For $r = 2.0$, however, we always see an increase in conductivity with temperature. In this case, $\mu(0)$ is in the gap, and all the temperature dependence of the dc conductivity is from the activation of carriers into the host band. The difference between Figure 2.10a and Figure 2.10b is that for larger $\Delta\varepsilon$, the temperature at which $\sigma(T)$ starts to increase
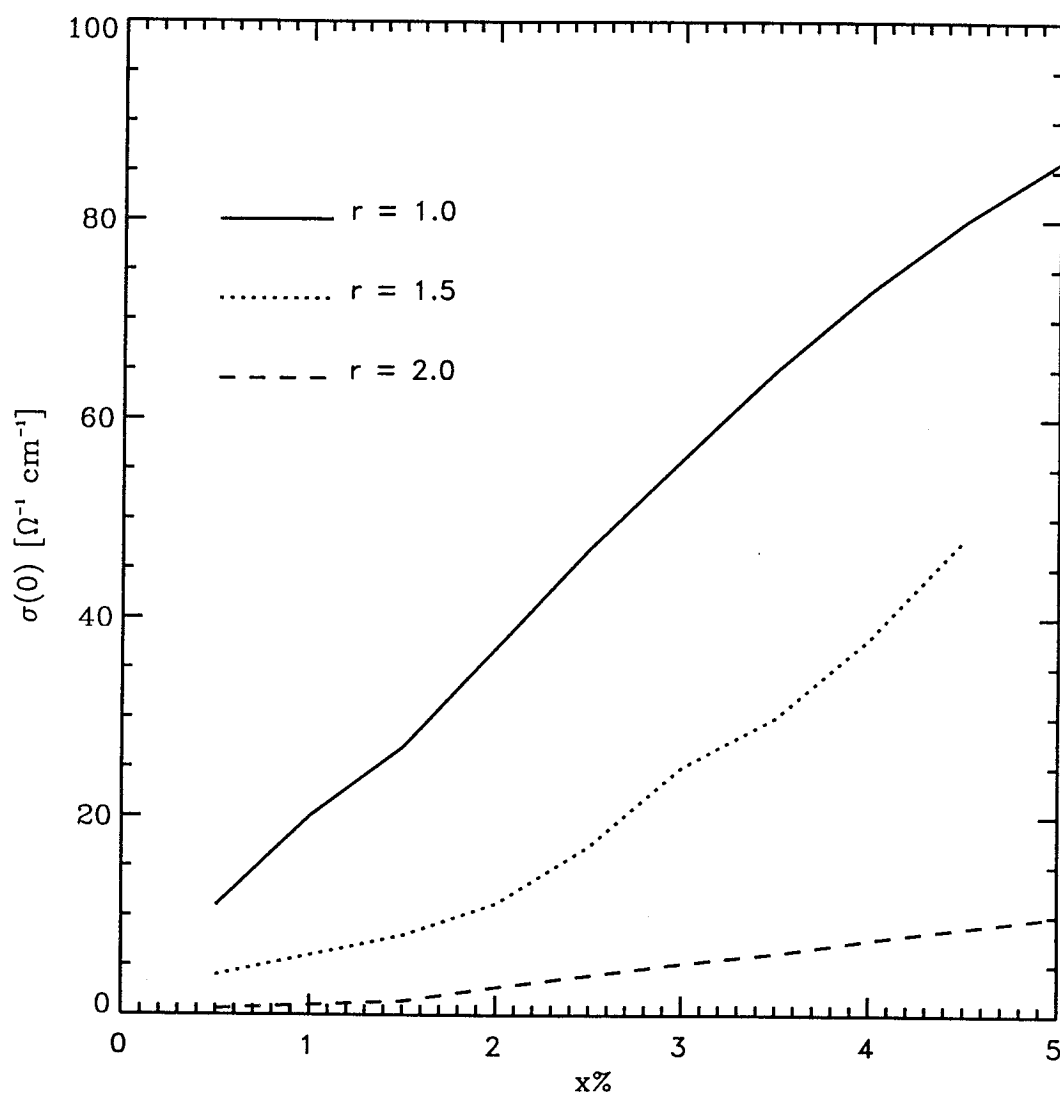
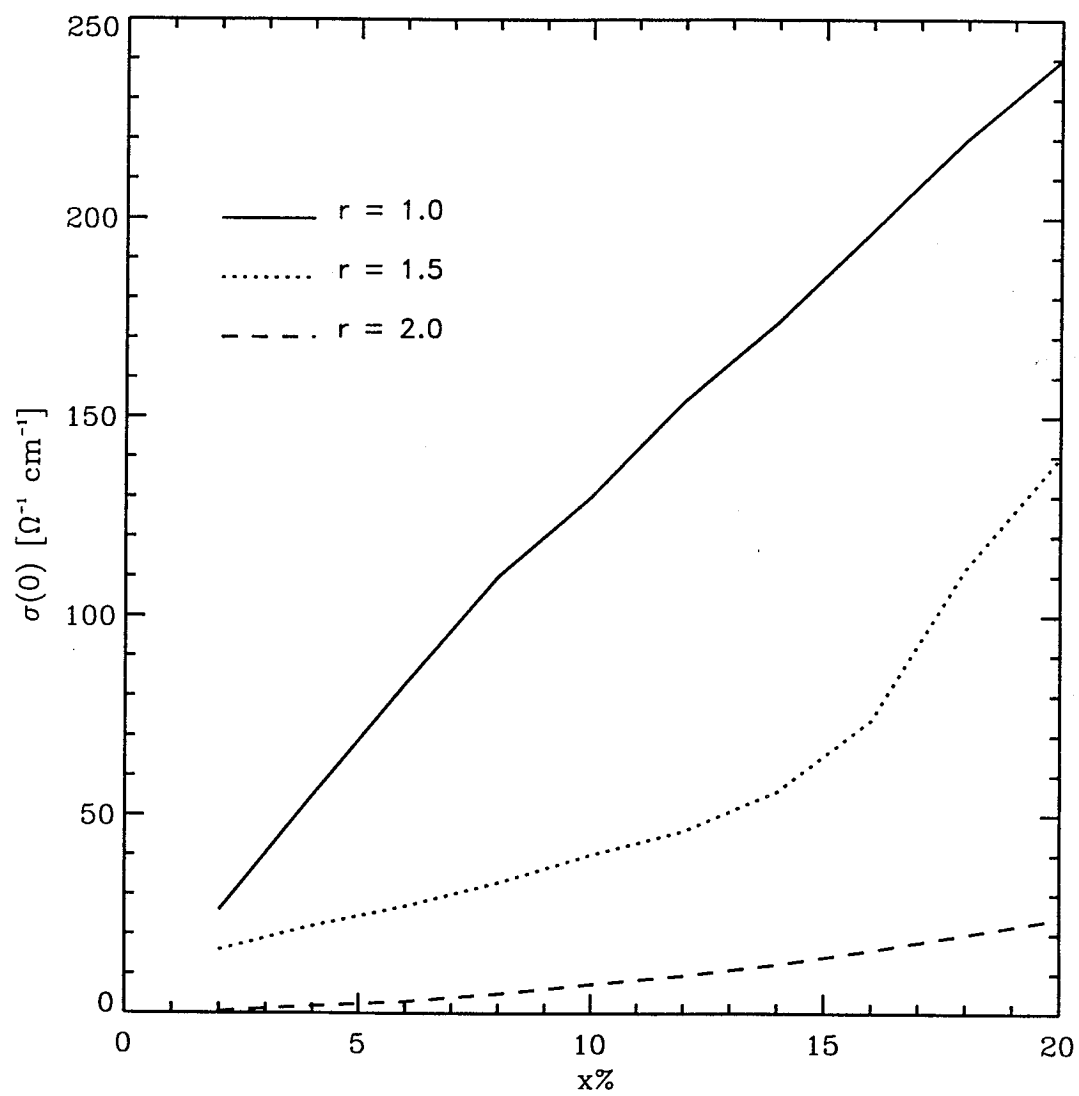Figure 2.9a $\sigma(0)$ as a function of x for $\Delta\epsilon = 0.85$ eV

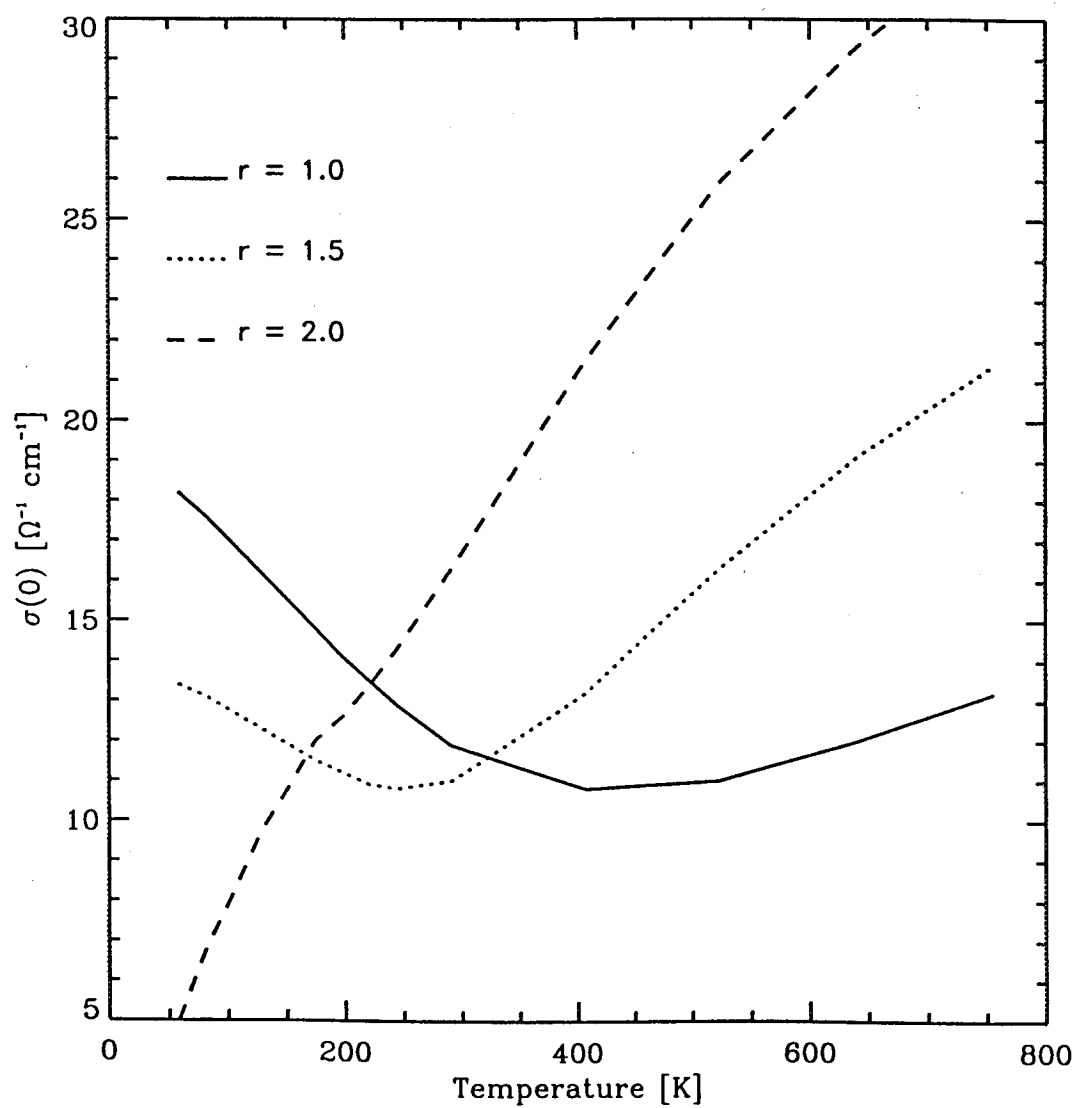Figure 2.9b $\sigma(0)$ as a function of x for $\Delta\epsilon = 1.1$ eV

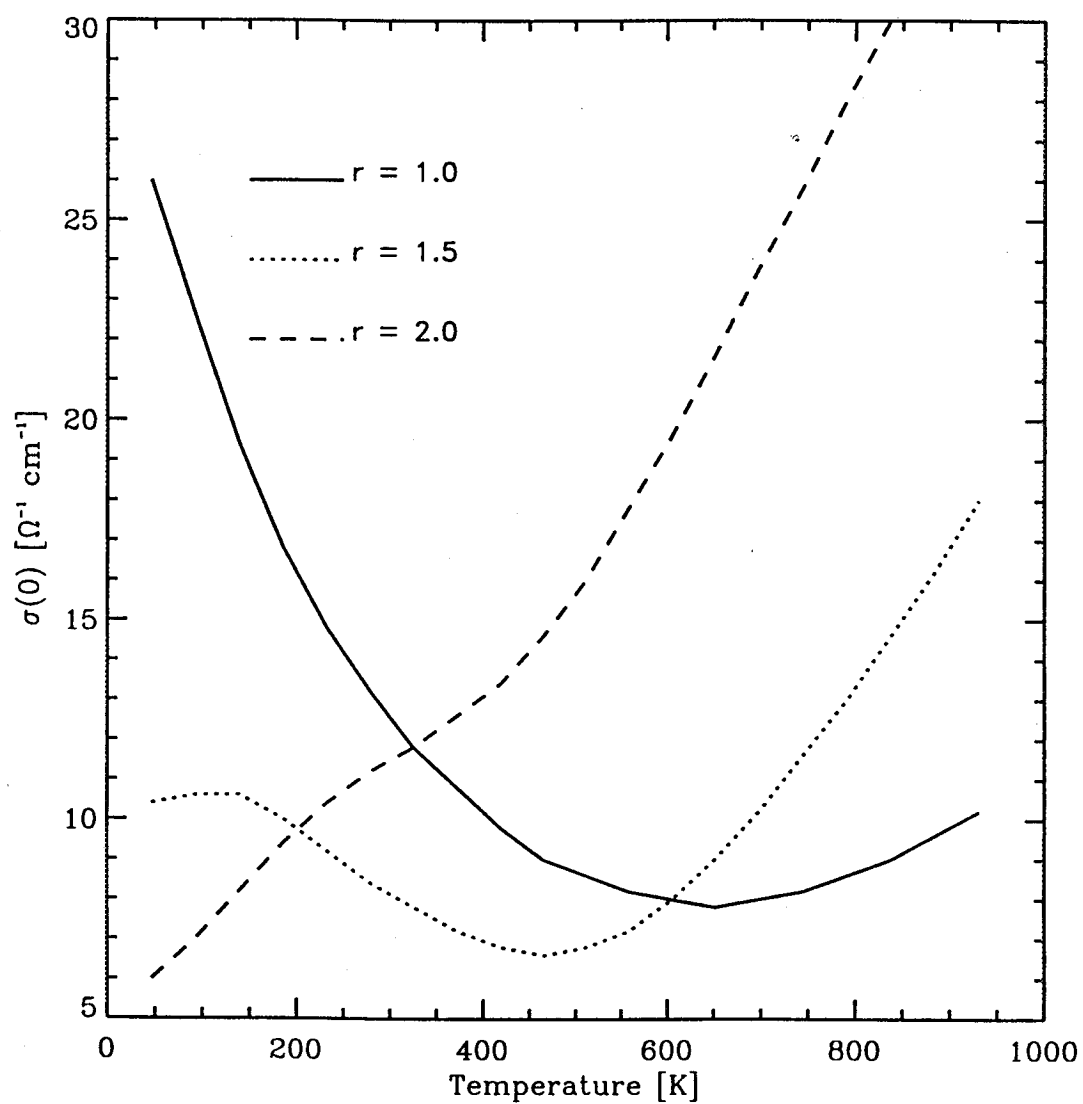Figure 2.10a $\sigma(T)$ as a function of T for $\Delta\epsilon = 0.85$ eV, x = 0.02

Figure 2.10b $\sigma(T)$ as a function of T for $\Delta\epsilon = 1.1$ eV, x = 0.02

with T is higher than that for smaller $\Delta\varepsilon$. Since for a larger $\Delta\varepsilon$, the activation energy is larger, we expect that a higher temperature will be needed to increase $\sigma(T)$ when activation is a dominated mechanism.

Although in Figure 2.10a and Figure 2.10b, we only showed our calculated $\sigma(T)$ for one defect concentration, we also did the calculation for other defect concentrations. For low concentration, because the states have low mobility, the main contribution to $\sigma(T)$ is from activation, so $\sigma(T)$ increases with T just as in intrinsic semiconductors. At higher concentration, on the other hand, because all the states have higher mobility, $\sigma(T)$ is dominated by states within the impurity band at low temperatures. When this is true $\sigma(T)$ decreases due to the shift in $\mu(T)$ for r=1.0 and 1.5.

For liquid semiconductors, because the defect concentration is expected to depend strongly on temperature, the temperature dependence of $\sigma(T)$ is may be dominated by the dependence of x on T. Because the melting temperature is already high (usually over 700 K), an increase of 50-100 K will not make a large difference in the conductivity due to thermal smearing alone. Figure 2.11 gives the dc conductivity as a function of $T\text{-}T_m$, where T_m is the melting temperature, and for three different values of $\mu(0)$. Because we do not know the relation between defect concentration and temperature, x has been assumed to be proportional to $T\text{-}T_m$. For $r = 2.0$, the conductivity increases with x almost linearly. But for $r = 1.0$ and 1.5, we can see that the conductivity increases at a lower rate for small $T\text{-}T_m$, while a higher rate is seen for larger $T\text{-}T_m$. Two different slopes can be clearly seen.

2.5. Thermopower $S(T)$

The calculation of thermopower is straightforward. By using our calculated $\mu(T)$ and $\sigma(T)$ we are able to include all temperature-dependent factors in the thermopower. Here again we are interested in the behavior of three different values of the Fermi energy, $\mu(0)$.

For $\mu(0)$ at the center of the defect band ($r = 1.0$), the thermopower (in $\mu V/K$) for different defect concentration between $x = 0.01$ and $x = 0.05$ is plotted in Figures 2.12a-d as a function of temperature. Note that the vertical scale is different for each of the figures. For all concentrations the thermopower is positive and increases with temperature, but at low temperature, $S(T)$ increases more slowly than at higher temperature. One can clearly see that with increasing concentration, the temperature region over which S increases slowly broadens. This corresponds to the calculated
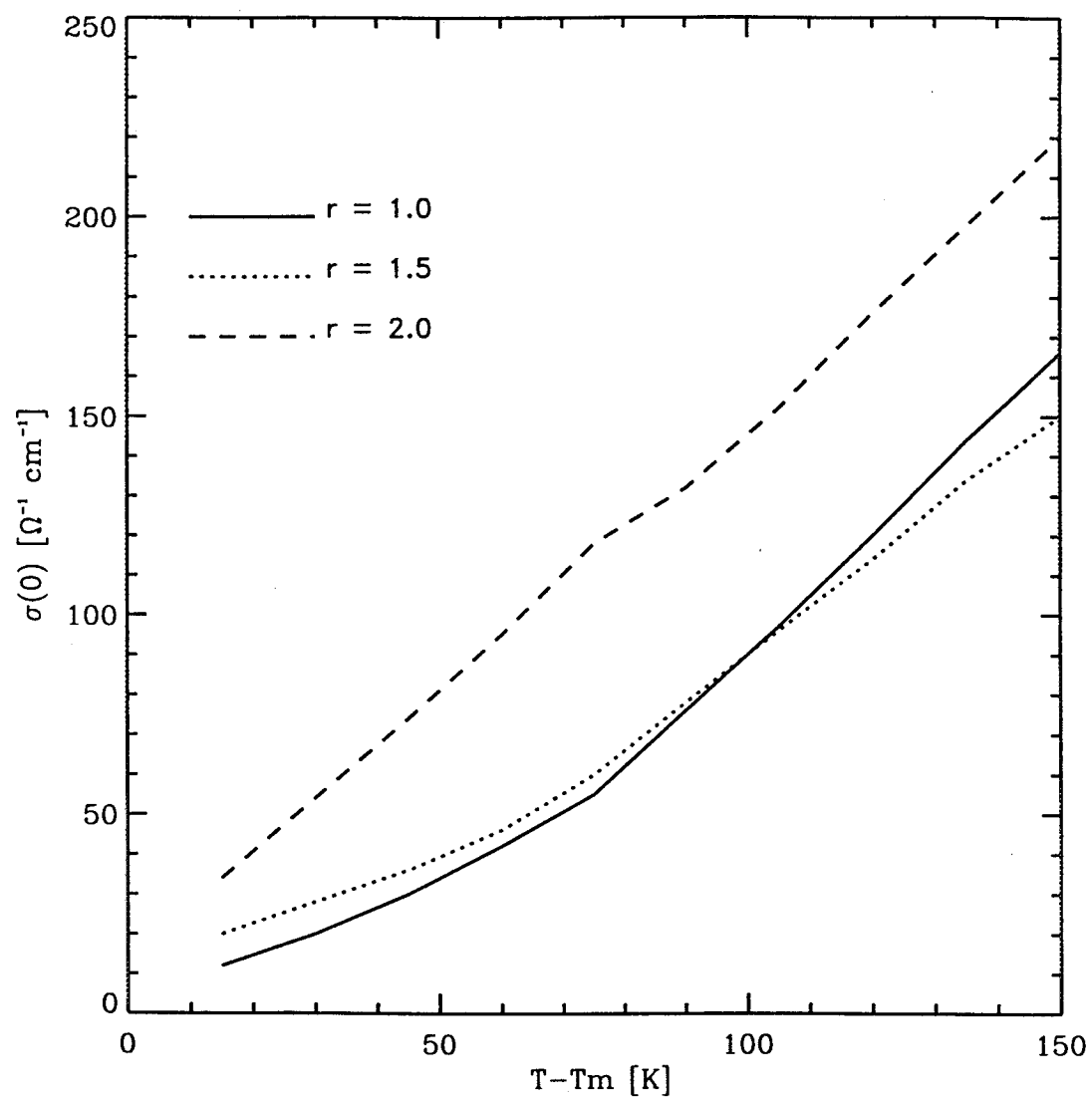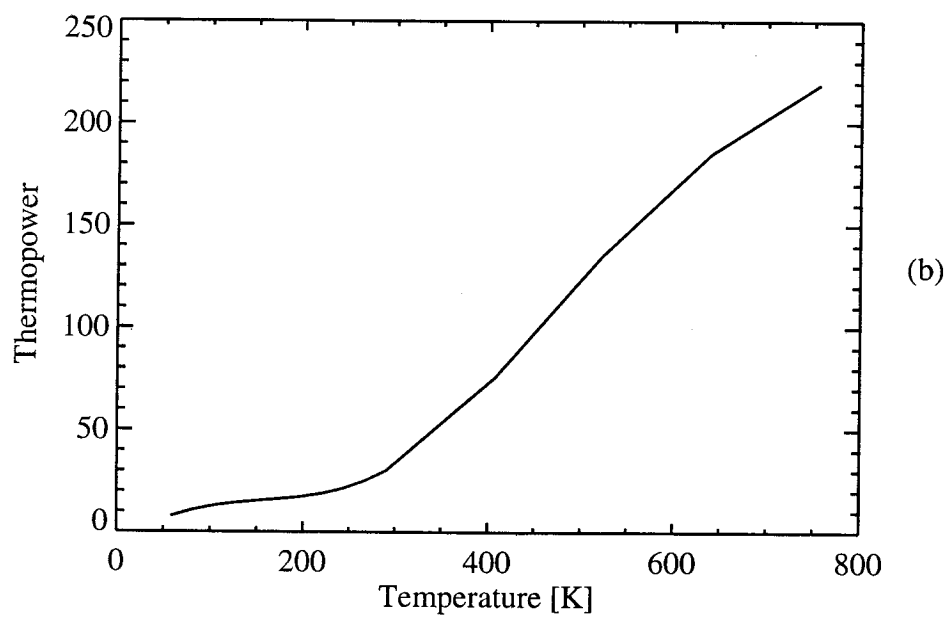
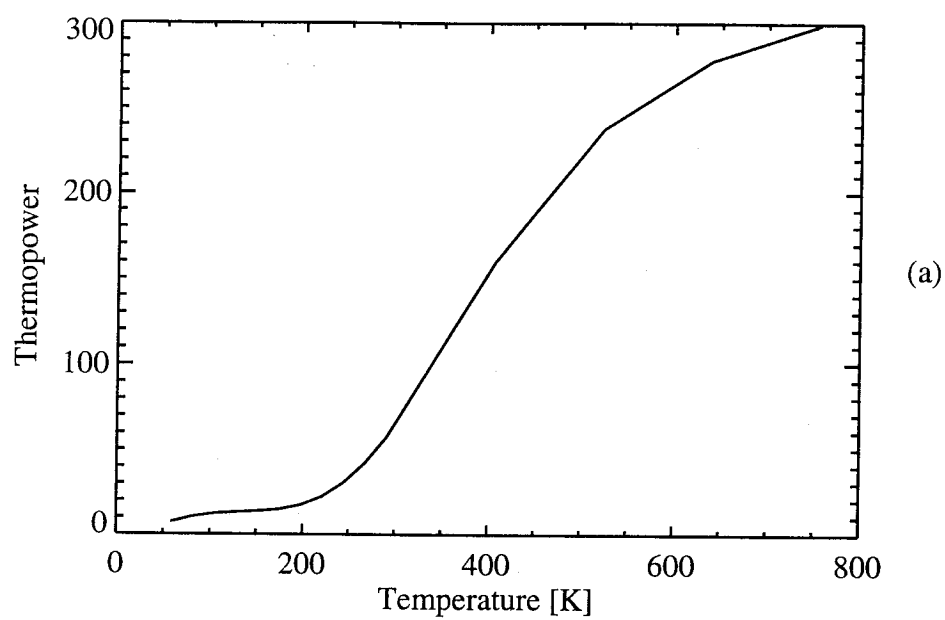Figure 2.11 $\sigma(T)$ as a function of T–Tm

(a)

(b)

Figure 2.12a,b Thermopower as a function of temperature for r=1.0.
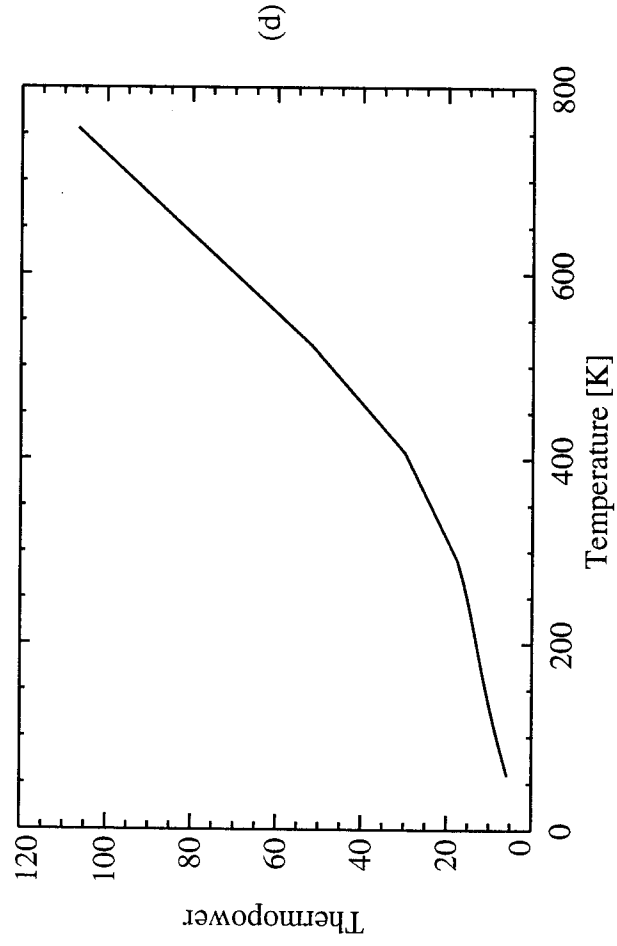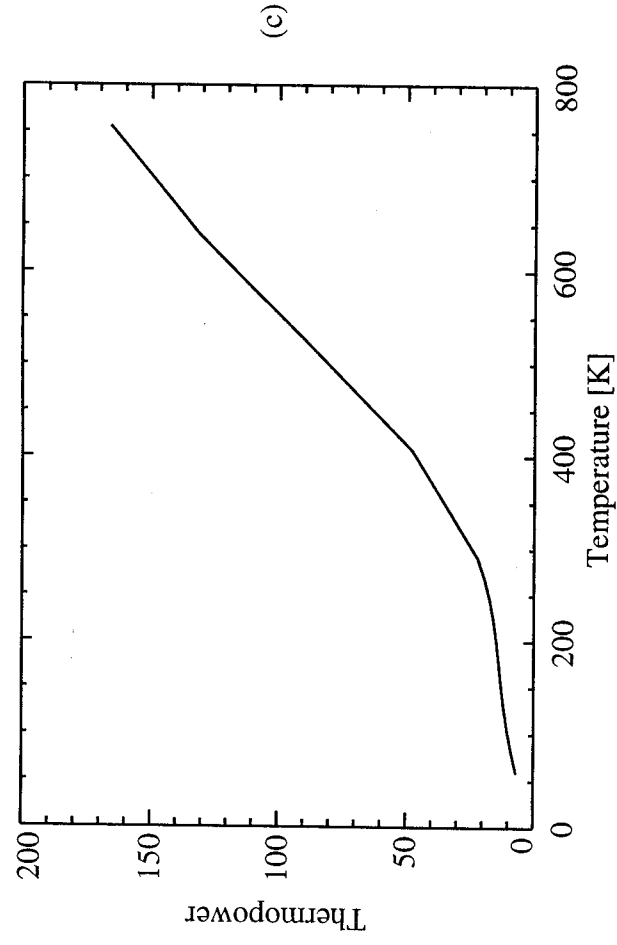(a) x=0.04, (b) x=0.05.

(c)

(d)

Figure 2.12c,d Thermopower as a function of temperature for r=1.0.
(c) x=0.04, (d) x=0.05.

behavior of $\mu(T)$ with T (see Figure 6.3a); at low temperature, there is essentially no shift of $\mu(T)$, but with increasing T, the shift in $\mu(T)$ grows.

For $\mu(0)$ on the edge of the defect band ($r = 1.5$), the thermopower (in μV/K) is plotted as a function of temperature in Figures 2.13a-d for values of x between $x = 0.01$ and $x = 0.05$. Again the vertical scales differ. One can see now that with increasing temperature S(T) has a sign change. At low temperature, S is negative and decreasing with temperature. At higher temperature, $S(T)$ increases with T and at last becomes positive. This can be understood in terms of the special features of the shift in $\mu(T)$ (See Figure 6.3c) and the effect of thermal smearing. These figures show that with increasing temperature, a sign change of the thermopower can be achieved.

For $\mu(0)$ in the gap ($r = 2.0$), we present the calculated thermopower (in μV/K) in Figures 2.14a-d. As for r=1.0, we can see that S is positive, but now there are three different temperature regions. At low temperature, S increases; then in the immediate temperature region, it decreases with temperature. At even higher temperatures, S increases with temperature again but the slope is much smaller than at low temperature. This can also be understood in terms of the shift in $\mu(T)$ (See Figure 3.3b).

2.6. Thermopower as Function of Concentration in Binary Alloys.

Some alloys consist of components which differ greatly in electronegativity. These alloys exhibit interesting behavior because they have a gap in their density of states. Consider an A_xB_{1-x} alloy system. At the stoichiometric composition, the Fermi energy lies in the middle of the gap, because the number of electrons contributed by the more electropositive component just equals the number of holes in the band of the more electronegative component. For other concentrations, the behavior of the Fermi energy is shown schematically in Figure 2.15. When a small amount of A is added to B, electrons are transferred from B to A causing the Fermi energy to shift to a lower energy. One can see that with increasing concentration x, the Fermi energy moves from the B band to the A band, while the A band grows at the expense of the B band. The calculations presented in this dissertation support this model.

We have calculated the thermopower and conductivity as a function of x for $\Delta\varepsilon = 1.9$ eV and two temperatures, T = 1000 K and T = 1200 K. The results are presented in Figure 2.16a and 2.16b. One can see that the conductivity has a minimum when the concentration reaches the stoichiometric value, while the thermopower changes sign at that point. Our model can only be expected to yield

(a)

(b)
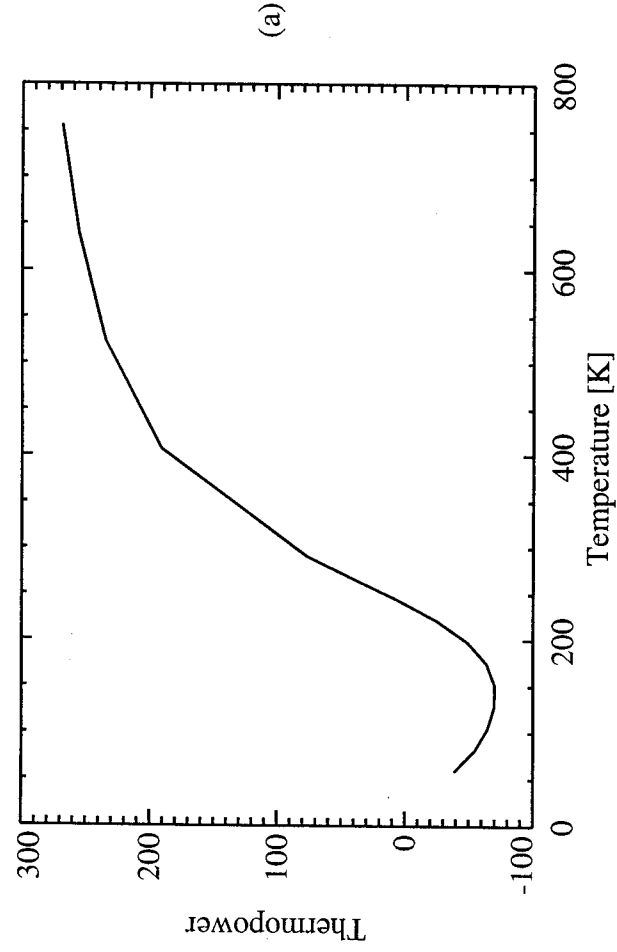
Figure 2.13a,bThermopower as a function of temperature for r=1.5.
(a) x=0.01, (b) x=0.02.

(c)

(d)
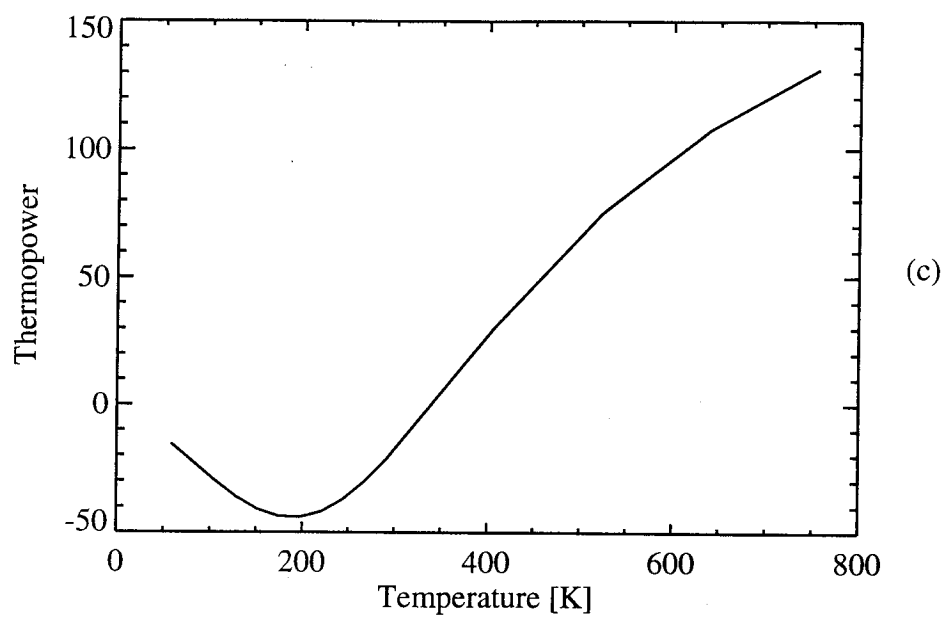
Figure 2.13c,d Thermopower as a function of temperature for r=1.5.

(c) x=0.04, (d) x=0.05.

(c)

(d)
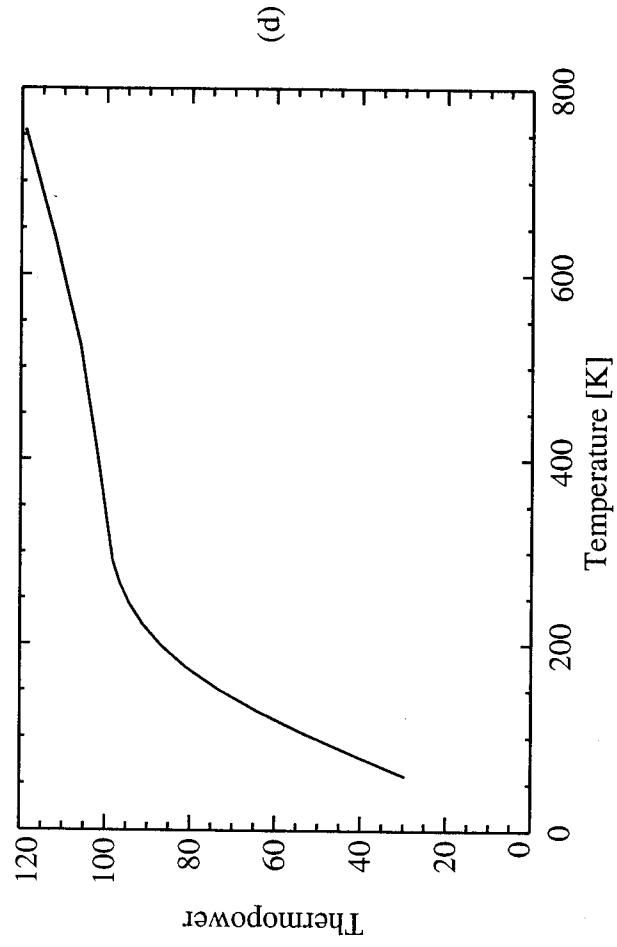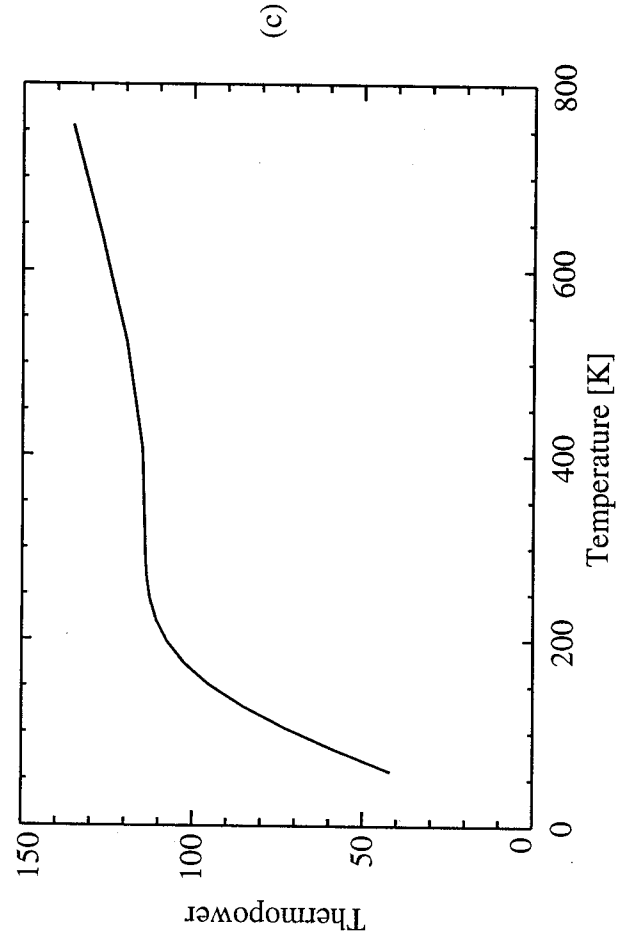
Figure 2.14c,d Thermopower as a function of temperature for r=2.0.

(c) x=0.04, (d) x=0.05.
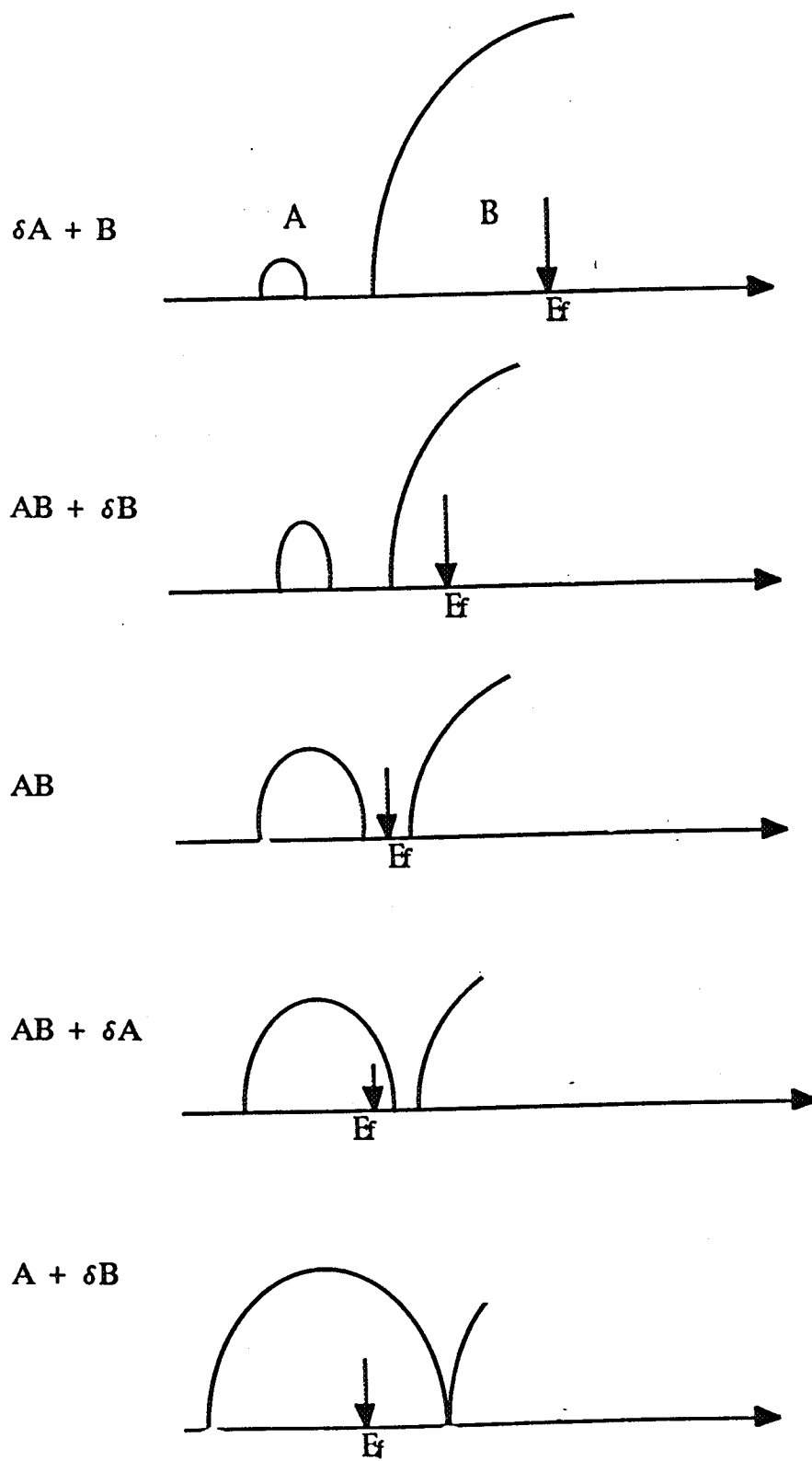
Figure 2.15 Schematical position of the Fermi level in the alloy.

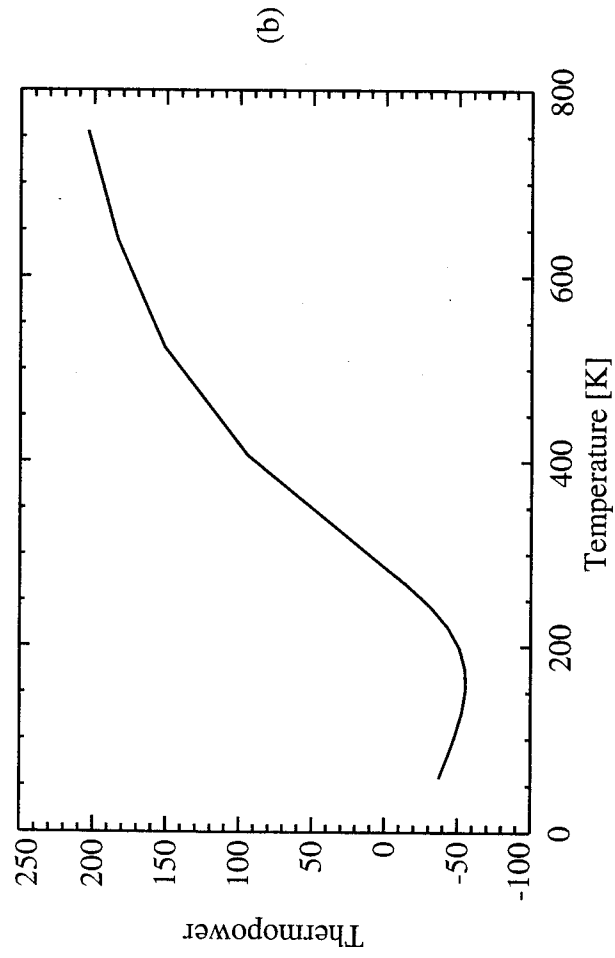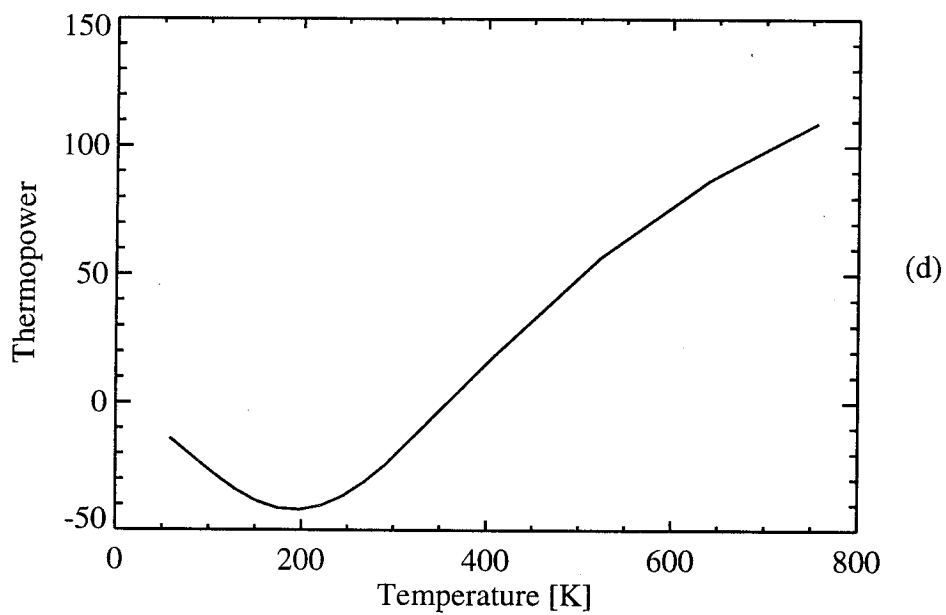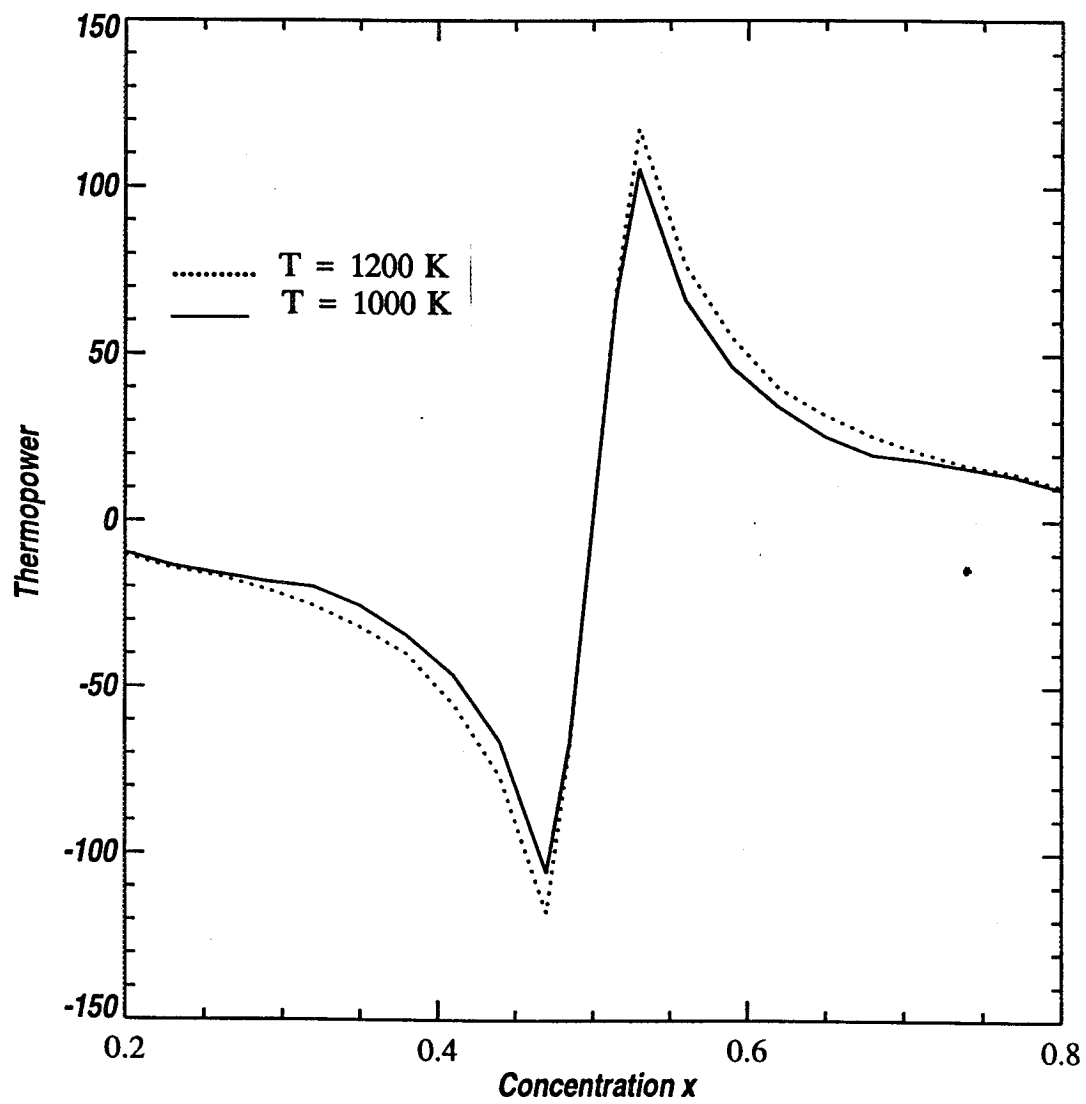Figure 2.16a Thermopower as a function of concentration for $\Delta\varepsilon = 1.9$ eV.
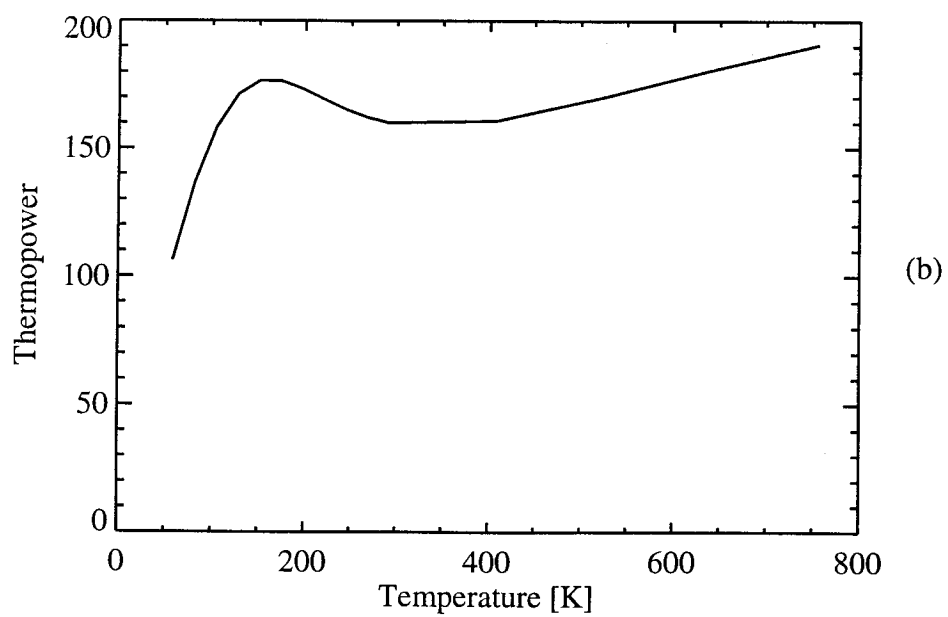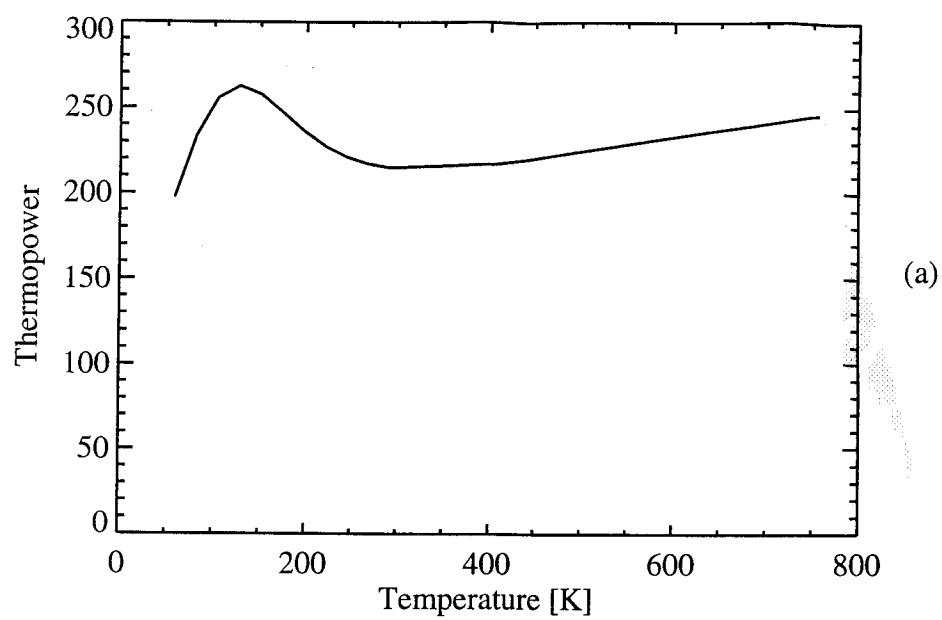
Figure 2.14a,b Thermopower as a function of temperature for r=2.0.

(a) x=0.01, (b) x=0.02.

Figure 2.16b Conductivity as a function of concentration for $\Delta\varepsilon = 1.9$ eV.

quantitative results in the region of strong scattering. This occurs in the stoichiometric region, where a metal-non-metal transition takes place, and the conductivity is less than about 400 $(\Omega$ cm$)^{-1}$. This corresponds to a concentration region between $x = 0.35$ and 0.65, our model should work well.

DISCUSSION

3.1 The DC Conductivity

In the model we used in this dissertation (See Chapter I), we have emphasized the two cases, small and large site energy differences, in Figure 1.1b-c. Figure 3.1a and Figure 3.1b show the calculated conductivity as a function of temperature for various defect concentrations for $\Delta \varepsilon = 0.85$ eV, and Fermi energy at the center of the defect band ($r = 1.0$) and on the side of the defect band ($r = 1.5$), respectively. The defect concentration increases from $x = 0.01$ to $x = 0.05$ starting from the upper left corner and moving toward the lower right corner. Note the vertical scale range increases with concentration. We can see that for all temperatures the conductivity increases with increasing defect concentration. In addition, for all concentrations the conductivity decreases with increasing temperature at low temperature. At higher temperatures, on the other hand, the conductivity increases with increasing temperature. This is due to the shift of chemical potential and the effect of thermal smearing.

As pointed out in the introduction, the conductivity has two contributions, one from the carriers in the defect band $\sigma_{def}(T)$, another from the carriers excited to the host band $\sigma_{exc}(T)$. Therefore

$$\sigma(T) = \sigma_{def}(T) + \sigma_{exc}(T).$$

(3.1)

Figure 3.2a and Figure 3.2b show plots of $\sigma_{def}(T)/\sigma(T)$ as a function of T for $x=0.05$, three values of r (or $\mu(0)$) and $\Delta \varepsilon = 0.85$ eV, $\Delta \varepsilon = 1.1$ eV, respectively. One can see that at low temperature since $\mu(0)$ is in the defect band for r = 1.0 and 1.5, the ratio is about 1. Thus the dc conductivity is is dominated by carriers in the defect band as one would expect. With increasing temperature, carriers are excited to the host band and the ratio decreases. When $\mu(0)$ is in the gap (r = 2.0), the contribution from carriers in the defect band is very low at low temperature. With increasing temperature, this contribution increases, but the main contribution still comes from the host band. The increase occurs because the chemical potential shifts toward the defect band. The difference between Figure 3.2a and Figure 3.2b is that the latter one corresponds to a larger activation energy, and therefore changes occur in different temperature regions.

39
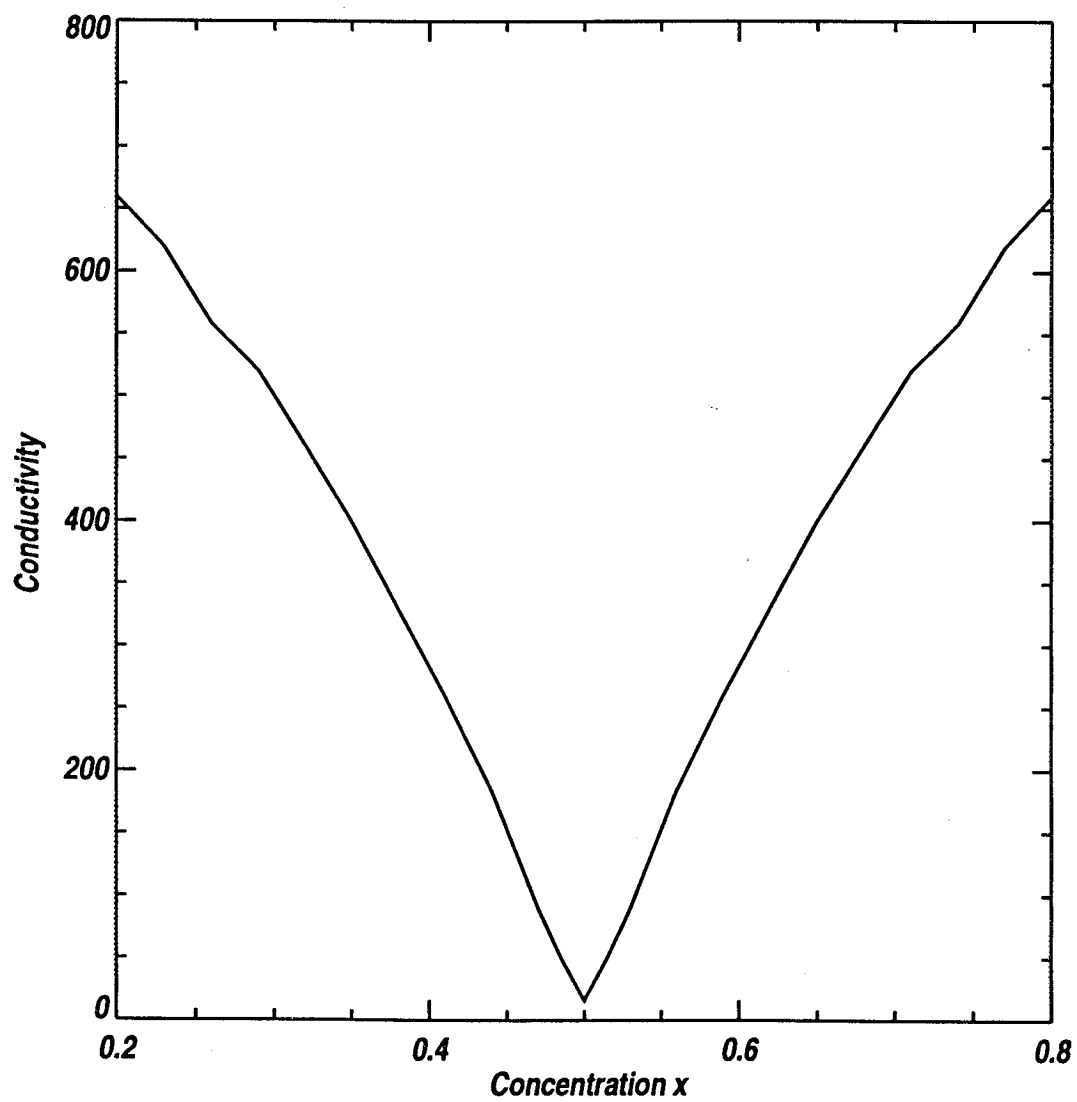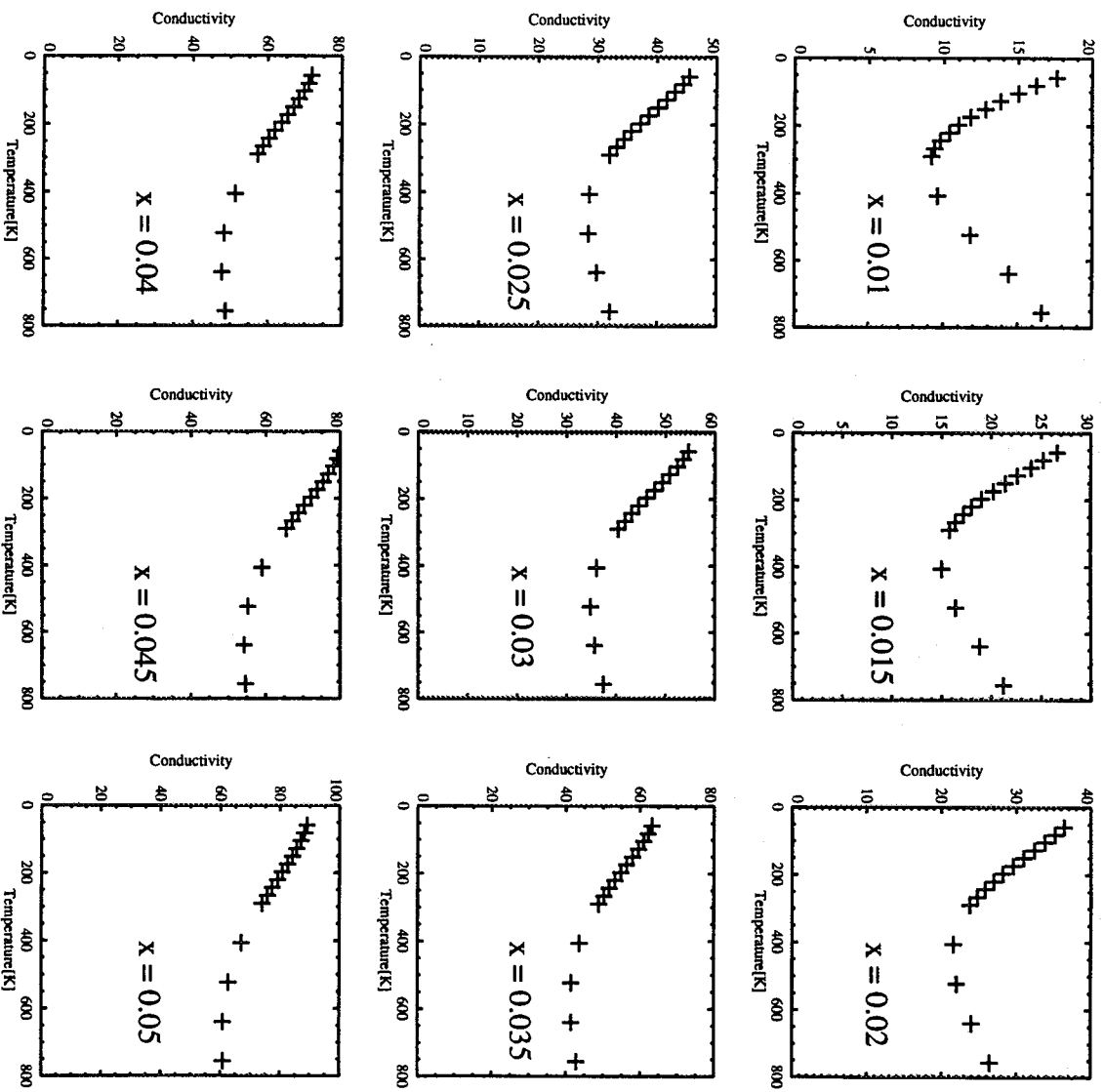
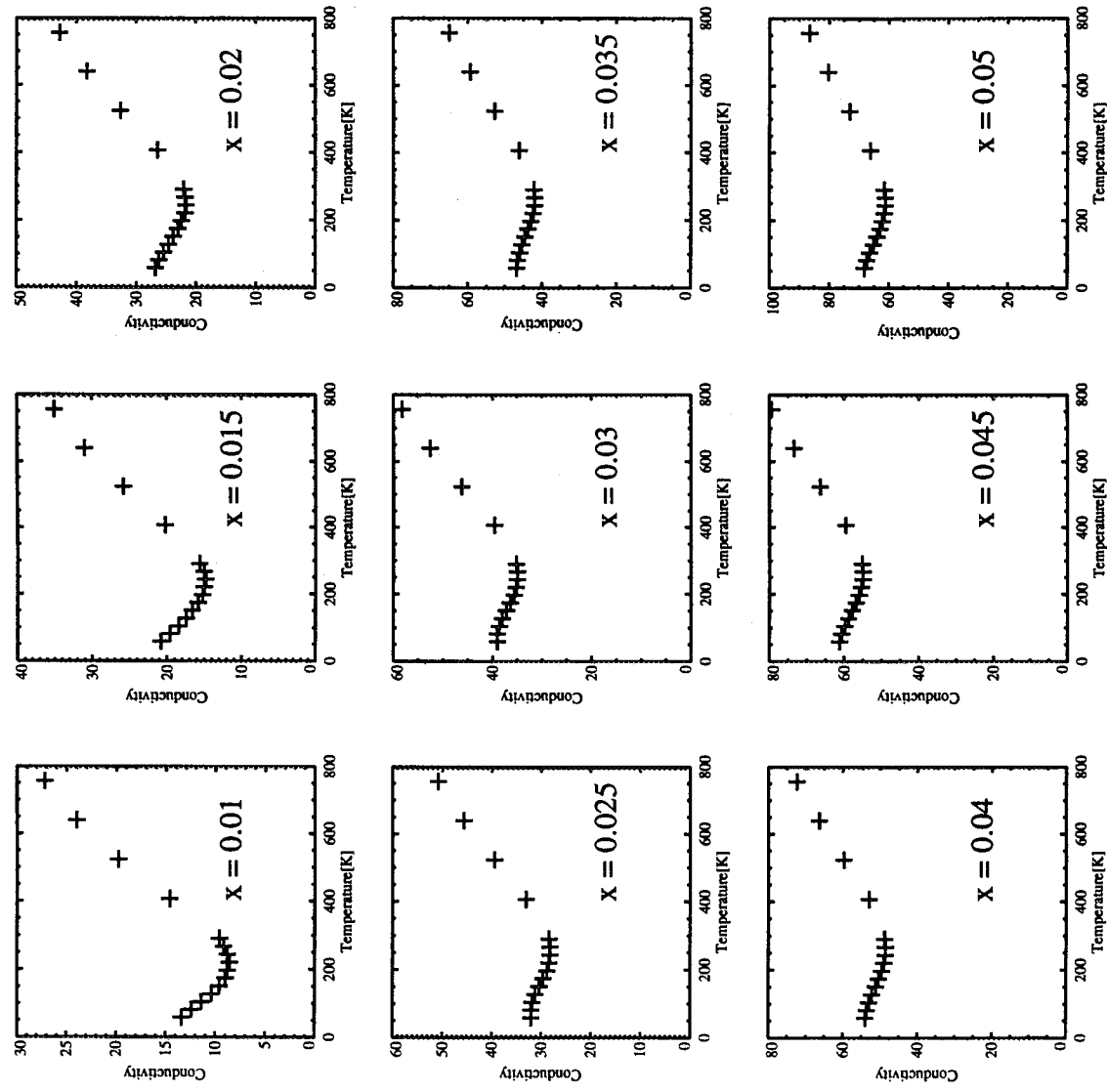Figure 3.1a Conductivity as a function of temperature for r=1.0.

Figure 3.1b Conductivity as a function of temperature for r=1.5.
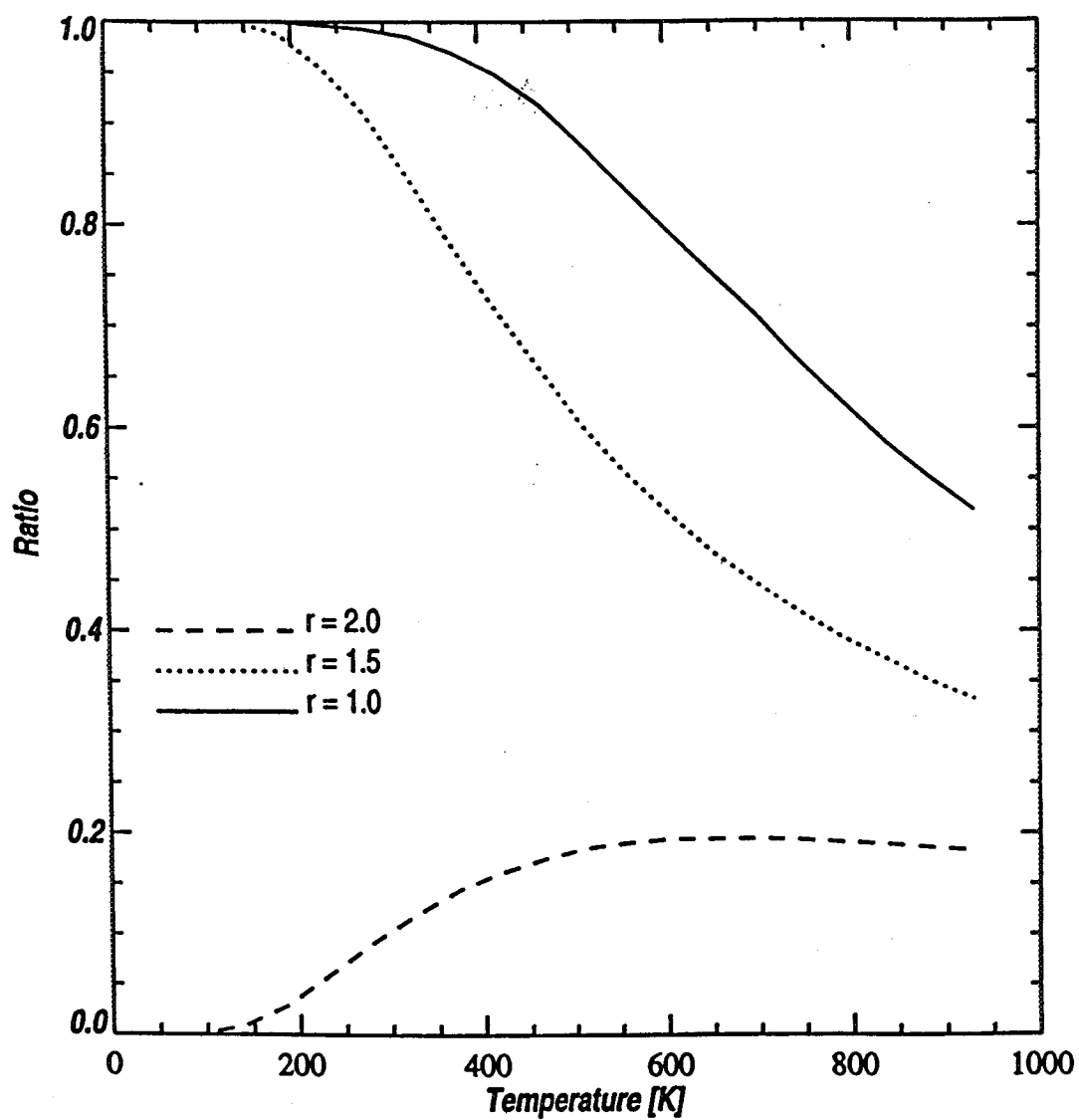
Figure 3.2a Ratio of the two part conductivity as a function of T for x = 0.05 and $\Delta \varepsilon = 0.85$ eV.
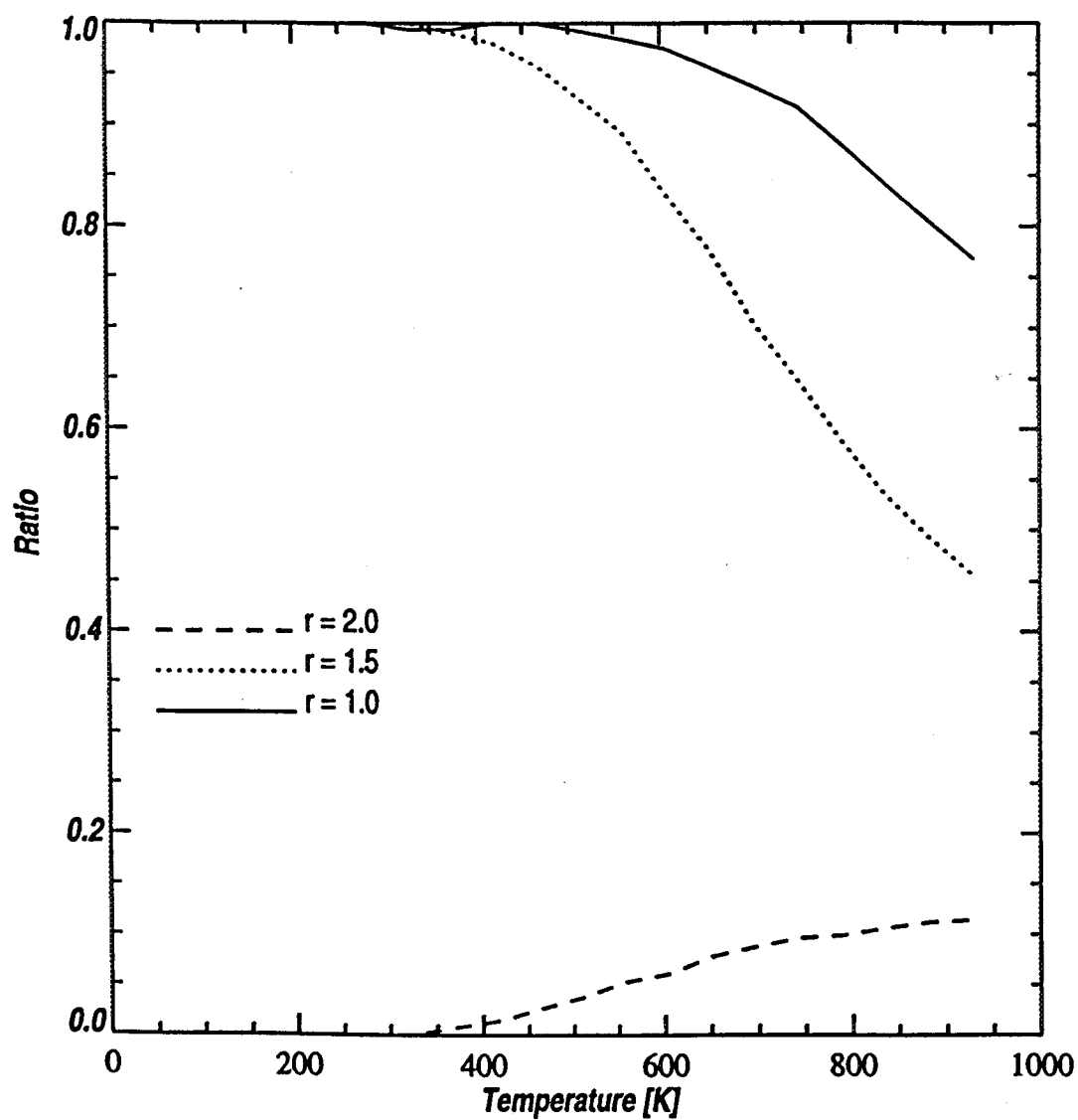
Figure 3.2b Ratio of the two part conductivity as a function of T for x = 0.05 and $\Delta\varepsilon = 1.1$ eV.

In Section 2.4, we have seen that when $\Delta\varepsilon = 1.1\ eV$, the calculation of conductivity is in agreement with the measured conductivity in II-VI semiconductor melts, both in order of magnitude and in the form of temperature dependence. For $\Delta\varepsilon = 0.85\ eV$, one can see that the calculated temperature dependence of the conductivity presented in Figure 3.1a and Figure 3.1b shows the same behavior as the measured conductivity in n-type silicon, i.e., the conductivity has a negative temperature coefficient at lower temperatures and a positive temperature coefficient at higher temperatures, and the order of magnitude is same as the measured values in most temperature regions. It should be pointed out, however, that the defect concentration used in this calculation are much higher than the impurity concentration in the silicon. This is because in real semiconductors, the dielectric constants ϵ_0 are large. For example, $\epsilon_0 = 16$ for Ge, and 12 for Si. In materials with large dielectric constants, the wavefunctions of the electrons at donor sites and holes at acceptor sites are highly extended. Because of this carriers can tunnel large distances and the effective nearest neighbor distance is greatly increased. In our calculation, we have taken $\epsilon_0 = 1$. The equivalent concentrations are expected to differ by a factor of $1/\epsilon_0^6$.

It is interesting to estimate the Hall mobility, $\mu_m(T)$, of the electrons in the two bands for different positions of the Fermi level (values of $\mu(0)$). The mobility is estimated in the following way.

$$\mu_m(T) = \sigma(T)/en_{band}(T), \tag{3.2}$$

where $n_{band}(T)$ is the number of electrons in the band. Figure 3.3a and Figure 3.3b exhibit the Hall mobility in the defect band as a function of temperature for $x=0.05$, and $\Delta\varepsilon = 0.85\ eV$ and $\Delta\varepsilon = 1.1\ eV$. The typical value of the mobility of a carrier in the defect band is 25 cm²/V·s, while for the carriers in the host band, the value of mobility is approximately 100 cm²/V·s. One can see that the mobility is the largest with $\mu(0)$ at the defect band center ($r = 1.0$), and the mobility of electrons in the defect band always decreases with temperature when $\mu(0)$ lies in the band (e.g. $r = 1.0$ and $r = 1.5$). When $\mu(0)$ is in the gap, the mobility of the carriers in the defect band increases with increasing temperature, but the value is smaller than when $\mu(0)$ is in the band. This helps us to understand the conductivity behavior in a more direct way.
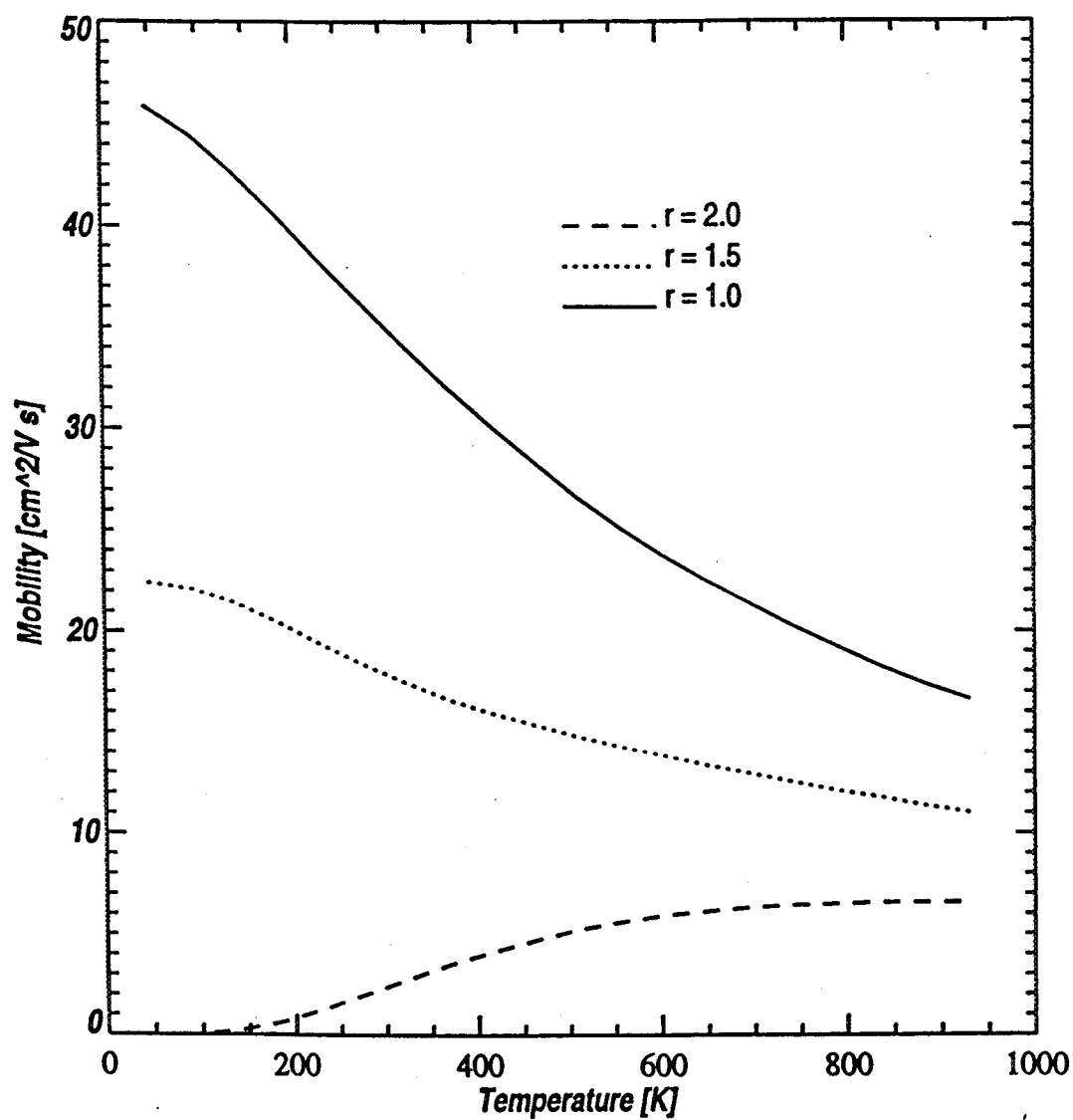
Figure 3.3a The carrier mobility as a function of T for x = 0.05 and Δε = 0.85 eV.
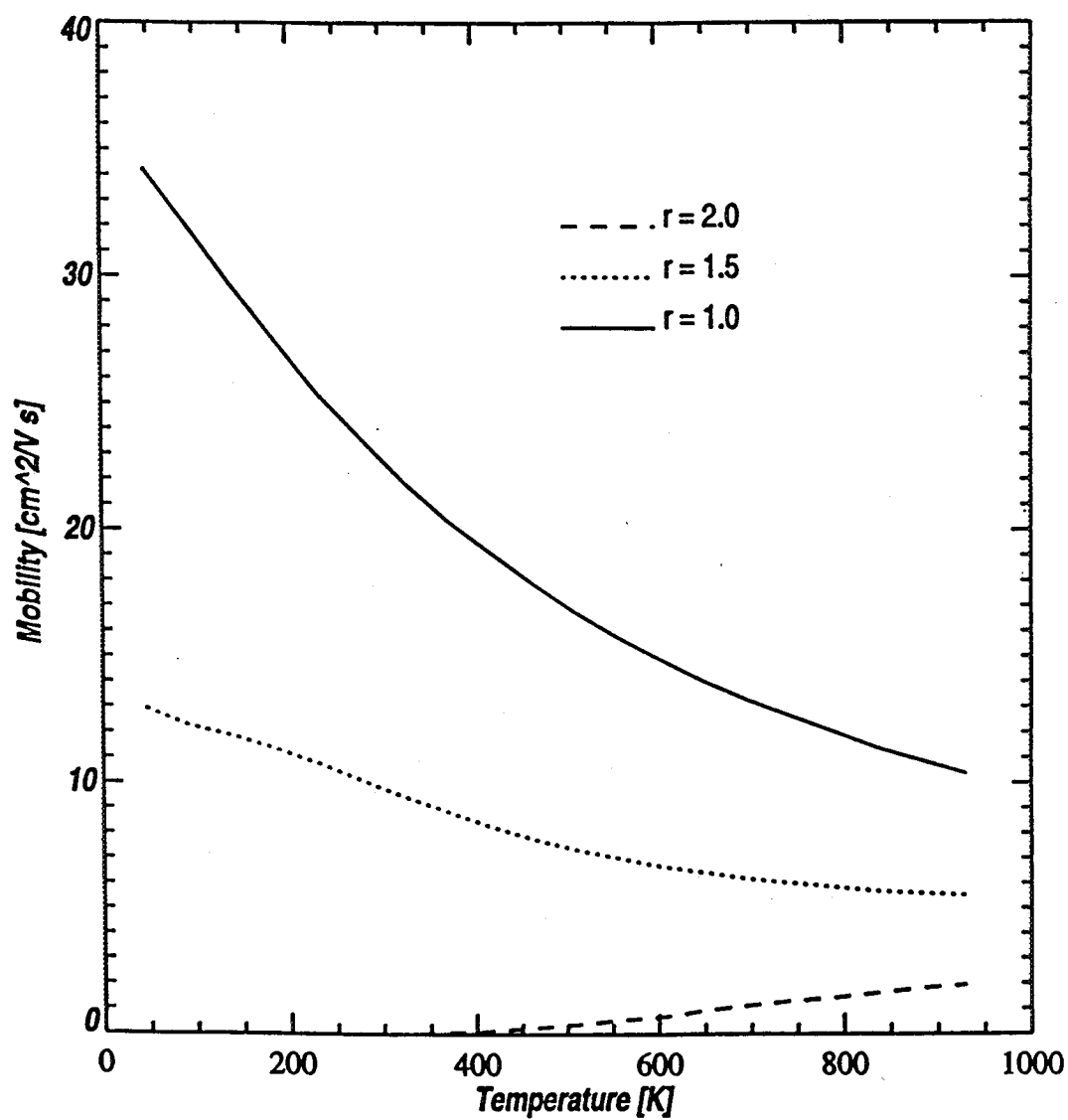
Figure 3.3b The carrier mobility as a function of T for x = 0.05 and $\Delta \varepsilon$ = 1.1 eV.

3.2. Thermopower

In the last section, we presented our calculation results of thermopower for amorphous and liquid systems. The results there are very general, but the temperature dependence of S is particularly interesting. In this section we compare our calculation to some experimental results.

3.2.1. Thermopower in Amorphous Semiconductors

The temperature dependence of the thermopower in a-Ge has not been explained, neither the order of magnitude nor the change of sign. (See Figure 2.5). From the point of this work, the sign change in thermopower is easily obtained when the Fermi level is near the down slope of a defect band. Figure 3.4 shows thermopower as a function of temperature for $x = 0.02$, and $r = 1.0, 1.5, 2.0$. One can see that when the Fermi energy sits either near the center of the defect band ($r=1$) or in the gap ($r=2.0$), the thermopower does not experience a sign change with increasing temperature. However, when the Fermi energy lies on the side (e. g. $r=1.5$) of the defect band, a sign change occurs, and the value of thermopower is the same order of magnitude as for a-Ge.

3.2.2. Thermopower in alloys near the metal-non-metal transition composition

Experimental measurement of thermopower in alloys show many different characteristics. For example, in the liquid Mg-Bi system, the thermopower curve is very smooth as a function of concentration and the value is relatively large near the stoichiometric composition. In liquid Mg-Sb, on the other hand, the thermopower varies rapidly with concentration and the sign changes at the stoichiometric concentration. This behavior can not been explained with the Barnes-Enderby model. The weak point of the model is that there is no way to calculate the DOS and $\sigma(E)$, so to locate the Fermi energy is very difficult. this makes it impossible to determine the shift of chemical potential with temperature. What Barnes and Enderby did was to assume that an energy gapexisted. Then by also assuming that the conductivity was due to activataion across this gap, they were able to determine the size of the gap and the position of the Fermi energy by measuring the conductivity at different temperatures. They also assumed that the conductivity was a linear function of energy near the band edge. Finally, they ignored the temperature dependence of the chemical potential.

In our calculation, however, we are able to locate the Fermi energy accurately. As the concentration varies, our calculation shosd that the Fermi energy can move from one band through the gap and into the other band, rather than always remaining in the gap as assumed in the Barnes-Enderby model.
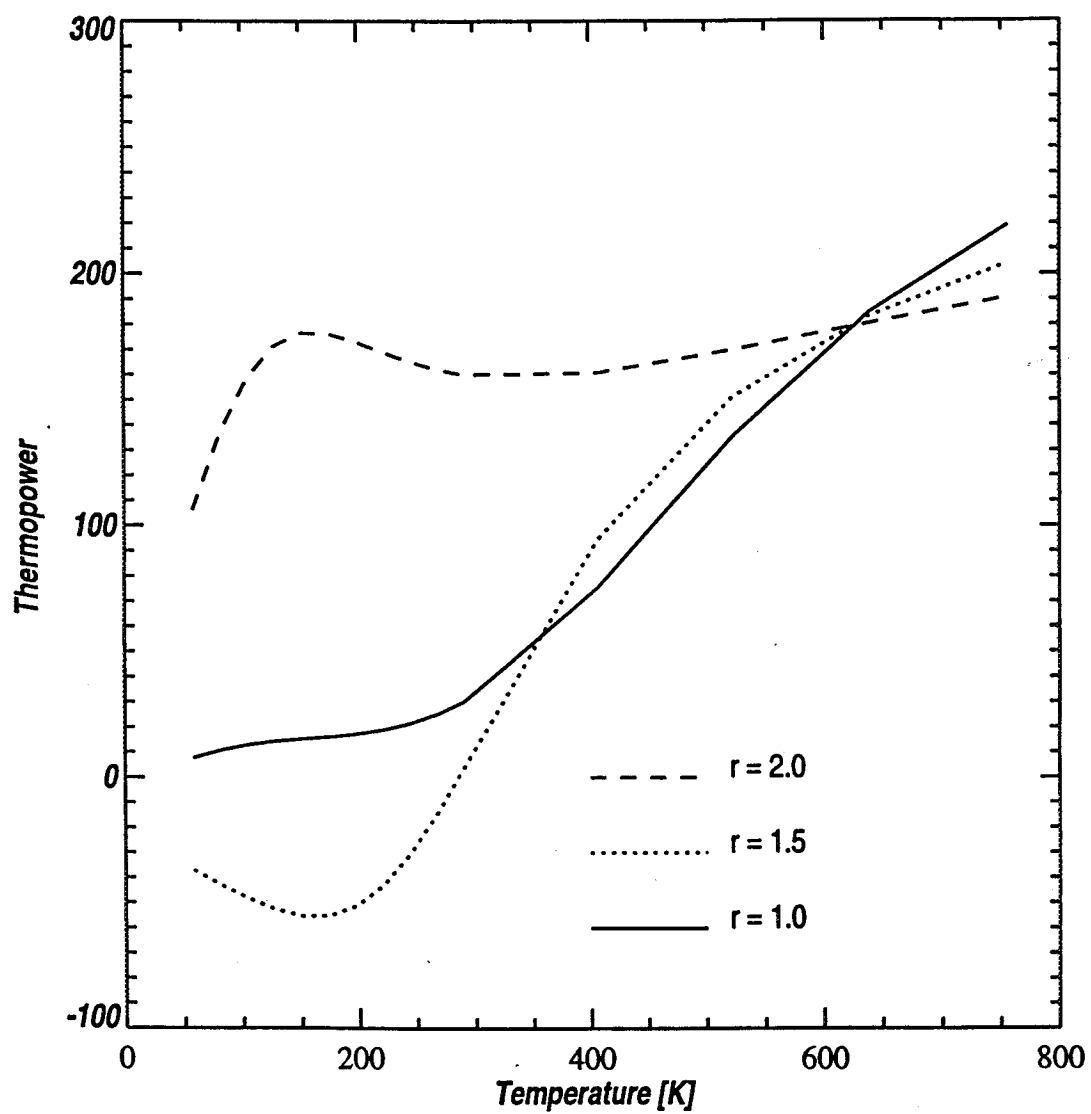
Figure 3.4 Thermopower as a function of temperature for x=0.02.

In Mg:Sb the electronegativity is sufficiently large that a gap opens between the bands, and we can use our model to calculate the thermopower. We calculated the thermopower for $\Delta \varepsilon = 1.5$ eV. The result is presented in Figure 3.5. By comparison with Figure 2.16a, one can see that the variation in the calculated thermopower is sharper but the order of magnitude is the same as the measured value.

Figure 3.5 Thermopower as a function of concentration x for $\Delta\varepsilon$ = 1.5 eV and T = 1000K.

NASA
National Aeronautical and Space Agency

Report Document Page

1. Report No. Final	2. Government Accession No.	3. Recipient's Catalog No.	
4. Title and Subtitle Computational MOdeling of Properties		**5. Report Due** 7/11/94	
		6. Performing Organization Code University of Alabama in Huntsville	
7. Aurthor(s) Judy R. Franz		**8. Performing Organization Report No.**	
		10. Work Unit No.	
9. Performing Organization Name and Address Department of Physics University of Alabama in Huntsville Huntsville, Alabama 35899		**11. Contract or Grant No.** NAS8-38609 D.O. 78	
12. Sponsoring Agency Name and Address National Aeronautics and Space Administration Washington, D.C. 20546-001 Marshall Space Flight Center, AL 35812		**13. Type of report and Period covered** Final 3/12/93 - 7/11/94	
		14. Sponsoring Agency Code	

15. Supplementary Notes

16. Abstract

A simple model was developed to calculate the electronic transport parameters in disordered semiconductors in strong scattered regime. The calculation is based on a Green function solution to Kubo equation for the energy-dependent conductivity. This solution together with a rigorous calculation of the temperature-dependent chemical potential allows the determination of the dc conductivity and the thermopower. For wide-gap semiconductors with single defect bands, these transport properties are investigated as a function of defect concentration, defect energy, Fermi level, and t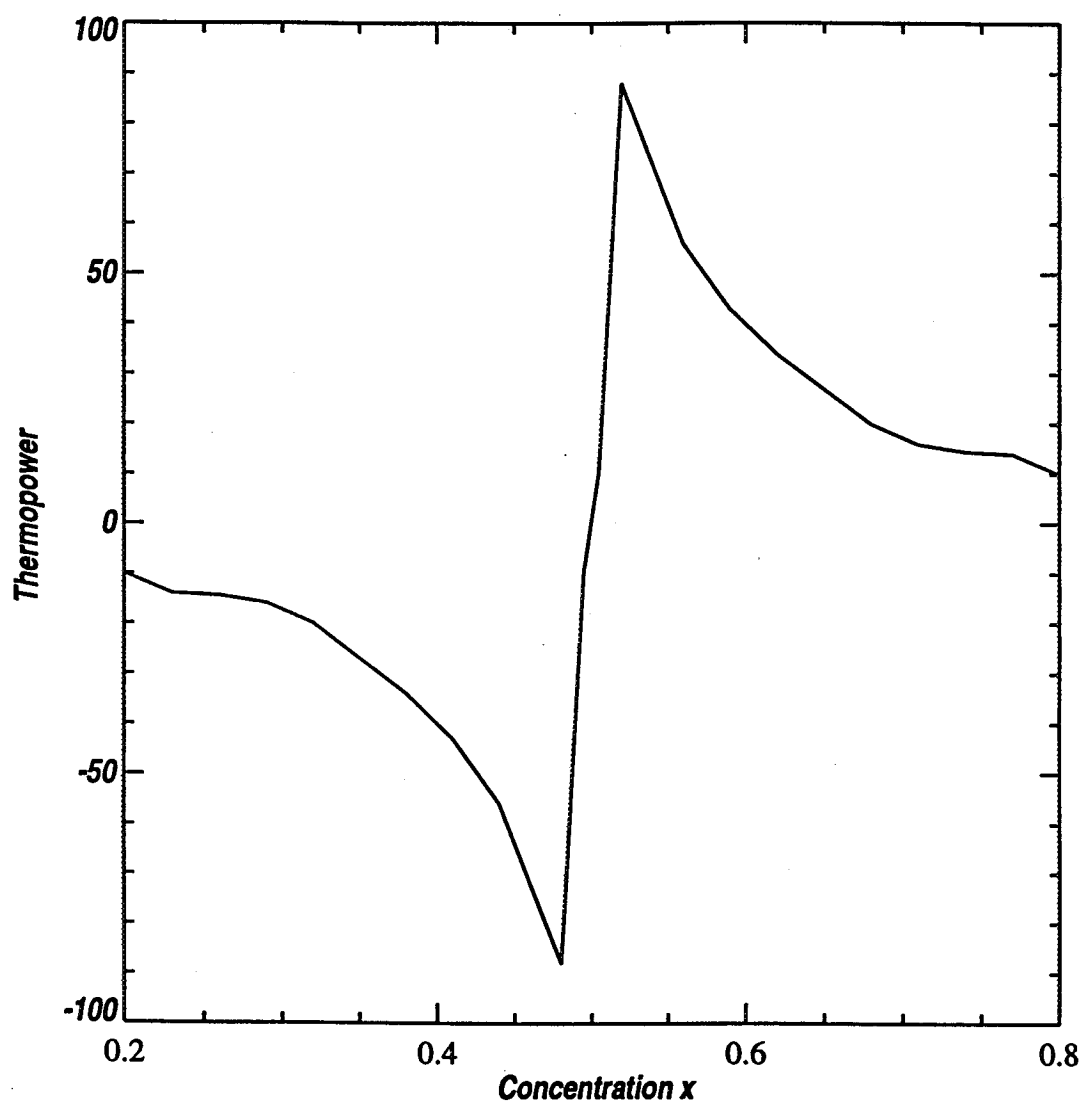emperature. Under certain conditions the calculated conductivity is quite similar to the measured conductivity in liquid II-VI semiconductors in that two distinct temperature regimes are found. Under different conditions the conductivity is found to decrease with temperature; this result agrees with measurements in amorphous Si. Finally the calculated thermopower can be positive or negative and may change sign with temperature or defect concentration.

17. Key Words (Suggested by Author(s)) Semiconductors, conductivity, thermo- power	**18. Distribution Statement** Unclassified - unlimited		
19. Security Class. (of this report) Unclassified	**20. Security Class. (of this page)** Unclassified	**21. No. of pages** 49	**22. Price**

NASA FORM 1626 OCT 86